Author/s:
Vuckovic, S;Vandyke, K;Rickards, DA;McCauley Winter, P;Brown, SHJ;Mitchell, TW;Liu, J;Lu, J;Askenase, PW;Yuriev, E;Capuano, B;Ramsland, PA;Hill, GR;Zannettino, ACW;Hutchinson, AT

Title:
The cationic small molecule GW4869 is cytotoxic to high phosphatidylserine-expressing myeloma cells

Date:
2017-05-01

Citation:
Vuckovic, S., Vandyke, K., Rickards, D. A., McCauley Winter, P., Brown, S. H. J., Mitchell, T. W., Liu, J., Lu, J., Askenase, P. W., Yuriev, E., Capuano, B., Ramsland, P. A., Hill, G. R., Zannettino, A. C. W. & Hutchinson, A. T. (2017). The cationic small molecule GW4869 is cytotoxic to high phosphatidylserine-expressing myeloma cells. British Journal of Haematology, 177 (3), pp.423-440. https://doi.org/10.1111/bjh.14561.

PROF. ANDREW CHRISTOPHER WILLIAM ZANNETTINO (Orcid ID : 0000-0003-2535-3729)



Received Date : 02-Oct-2016

Revised Date : 29-Nov-2016

Accepted Date : 01-Dec-2016

Article type : Ordinary Papers

# THE CATIONIC SMALL MOLECULE GW4869 IS CYTOTOXIC TO HIGH PHOSPHATIDYLSERINE-EXPRESSING MYELOMA CELLS

Slavica Vuckovic[1,2,3,†], Kate Vandyke[4,5,†], David A Rickards[6], Padraig McCauley Winter[6], Simon HJ Brown[7], Todd W Mitchell[7], Jun Liu[8], Jun Lu[8], Philip W Askenase[9], Elizabeth Yuriev[10], Ben Capuano[10], Paul A Ramsland[11,12,13,14], Geoffrey R Hill[1,15], Andrew CW Zannettino[4,5], and Andrew T Hutchinson[6,9,12]*

[1] The Bone Marrow Transplantation Laboratory, QIMR Berghofer Medical Research Institute, Brisbane, QLD 4006, Australia.

[2] School of Medicine, University of Queensland, Brisbane, QLD 4106, Australia.

[3] Mater Research, Translational Research Institute, Brisbane, QLD 4102, Australia.

[4] Faculty of Health Sciences, The University of Adelaide, Adelaide, SA 5005, Australia.

[5] Cancer Theme, South Australian Health and Medical Research Institute, Adelaide, SA 5000, Australia.

[6] School of Life Sciences, Centre for Health Technologies and the iThree Institute, University of Technology Sydney, Ultimo, NSW 2007, Australia.

[7] School of Biology and Illawarra Health and Medical Research Institute, University of Wollongong, Wollongong, NSW 2522, Australia.

[8] Department of Genetics, Yale Stem Cell Center, Yale Cancer Center and Yale Center for RNA Science and Medicine, New Haven, CT 06520, USA

[9] Section of Allergy and Clinical Immunology, Department of Internal Medicine, Yale School of Medicine, New Haven, CT 06520, USA.

[10] Medicinal Chemistry, Monash Institute of Pharmaceutical Sciences, Monash University, Parkville, VIC 3052 Australia.
[11] School of Science, RMIT University, Bundoora, VIC 3083, Australia.
[12] Centre for Biomedical Research, Burnet Institute, Melbourne, VIC 3004, Australia.
[13] Department of Immunology, Monash University, Alfred Medical Research and Education Precinct, Melbourne, VIC 3004, Australia.
[14] Department of Surgery Austin Health, University of Melbourne, Heidelberg, VIC 3084, Australia.
[15] Department of Bone Marrow Transplantation, The Royal Brisbane and Women's Hospital, Herston, QLD 4029, Australia.
† These authors contributed equally to this work

*Correspondence:
Dr A T Hutchinson
Research Department
Alexion Pharmaceuticals Inc.
New Haven
CT 06510
USA

Tel: +1 203 772 9673
Fax: +1 203 271 8196
E-Mail: ahutchinson82@gmail.com

Short title: Small molecule targeting of phosphatidylserine

Received 2 October 2016, accepted 1 December 2016



## ABSTRACT

We have discovered that a small cationic molecule, GW4869, is cytotoxic to a subset of myeloma cell lines and primary myeloma plasma cells. Biochemical analysis revealed that GW4869 binds to anionic phospholipids such as phosphatidylserine - a lipid normally confined to the intracellular side of the cell membrane. However, interestingly, phosphatidylserine was expressed on the surface of all myeloma cell lines tested (n=12) and 9/15 primary myeloma samples. Notably, the level of phosphatidylserine expression correlated well with sensitivity to GW4869. Inhibition of cell surface phosphatidylserine exposure with brefeldin A resulted in resistance to GW4869. Finally, GW4869 was shown to delay the growth of phosphatidylserine-high myeloma cells *in vivo*. To the best of our knowledge, this is the first example of using a small molecule to target phosphatidylserine on

malignant cells. This study may provide the rationale for the development of phosphatidylserine-targeting small molecules for the treatment of surface phosphatidylserine-expressing cancers.

**Key words:** GW4869/ multiple myeloma/ phosphatidylserine/ small molecule



## INTRODUCTION

Multiple myeloma (MM) is a malignancy characterised by the infiltration of clonotypic plasma cells in the bone marrow. Despite recent advances in treatment, MM remains incurable, and there is still an unmet need for novel therapeutic compounds. When identifying potential therapeutic targets in cancer, the majority of research has focused on proteins, such as signalling enzymes and integral membrane proteins. However, there is a growing appreciation that lipids may also represent attractive targets for cancer therapies. For example, glycolipids, such as various types of gangliosides, and Lewis antigens have been tested as targets in a clinical setting (Dingjan, *et al* 2015, Soliman, *et al* 2017), and the phosphocholine analogues edelfosine and perifosine, which are specific for lipid rafts and lead to alterations in cell surface receptor signalling, have also been assessed in clinical trials (Mollinedo and Gajate 2015, Nitulescu, *et al* 2016). Furthermore, phosphatidylserine (PS), a lipid normally confined to the cytoplasmic side of cell membranes, has emerged as a potential therapeutic target. For example, the novel anti-PS targeting therapeutic monoclonal antibody (mAb), bavituximab, has been evaluated in a number of clinical trials for solid tumours (DeRose, *et al* 2011, Digumarti, *et al* 2014). This is based on the finding that endothelial cells lining tumour blood vessels express cell surface (exoplasmic) PS. Thus, targeting the tumour vasculature with an anti-PS mAb is a potential mechanism to inhibit the growth of malignant cells (DeRose, *et al* 2011). In addition, it has been reported that some types of cancer cells, including glioblastoma, melanoma and various types of carcinomas, as well as blood cancer cell lines of myeloid and T cell leukaemia origin, express PS on their surface (Bankovic, *et al* 2013, Riedl, *et al* 2011, Schroder-Borm, *et al* 2005, Utsugi, *et al* 1991). Moreover, in some of these studies, cationic peptides have been proposed as potential therapeutics for their ability to preferentially bind to and lyse cell membranes enriched in anionic phospholipids such as PS (Bankovic, *et al* 2013, Schroder-Borm, *et al* 2005).

While screening for anti-MM compounds, we discovered that the small molecule, GW4869, was cytotoxic to a subset of MM cell lines and primary samples and inhibited the growth of RPMI-8226 cells in a xenograft model of MM. GW4869 is highly cationic and hydrophobic, and upon further analysis, we determined that GW4869 binds to membranes enriched in negatively charged lipids. This lead to the discovery that all MM cell lines and MM cells from approximately 60% of patients, express some level of cell surface PS. Interestingly, GW4869 has been described as an inhibitor of neutral sphingomyelinase 2 [nSMase2, also termed sphingomyelin phosphodiesterase 3 (SMPD3)] (Clarke and Hannun 2006, Marchesini, *et al* 2003), however we did not find evidence that GW4869 mediates MM cell cytotoxicity through this pathway. Instead, we found that the specific binding of GW4869 to PS led to gross cell membrane deformities, such as membrane ruffling, clustering of integral membrane proteins and reduced membrane fluidity, which may have contributed to the cytotoxic effects of the compound.

This study is the first to show that a large proportion of MM cells and cell lines express exoplasmic PS. Moreover, we also show, for the first time, that targeting PS with a small cationic molecule can lead to selective cell death of malignant cells. Therefore, our study provides the rationale for the development of anti-PS small molecules as novel therapies for surface PS-expressing cancers.

## METHODS

### Cell lines and primary samples

Daudi, HL-60, K562, Molt-4, NCI-H929 and RPMI-8226 cell lines were obtained from the American Type Culture Collection (ATCC; Manassas, VA, USA). JJN3, Jurkat, LP-1, OPM2 and U266 cell lines were obtained from the German Collection of Microorganisms and Cell Cultures GmbH (DSMZ; Braunschweig, Germany). No Short Tandem Repeat (STR) analysis was performed on these cell lines as they were obtained directly from the suppliers. ANBL6, Balm and Nalm-6 were obtained from Prof. Leonie Ashman (University of Newcastle, NSW). JIM1, KMS-11 and MM.1S were obtained from Prof. Andrew Spencer (Monash University, Melbourne). WL-2 was obtained from Prof. Douglas Joshua (RPA, Sydney) and KMS-18 was from Prof. Junia Melo (SA Pathology, Adelaide). The identities of KMS-11,

MM.1s and Nalm-6 were confirmed by STR analysis performed by the DNA Analysis Facility at Yale University (New Haven, CT, USA). No STR analysis was performed on ANBL6, Balm, JIM1, KMS-18 and WL-2, as at the time of the study, there was no available STR data to match these cell lines against. All cell lines were routinely tested for mycoplasma contamination. Peripheral blood mononuclear cells (PBMCs) were purified from the buffy coats of normal donors, provided by the Australian Red Cross Blood Service (Alexandria, NSW, Australia), by the Ficoll-Paque purification method. Primary bone marrow samples were collected, with informed consent, from randomly selected patients with newly diagnosed symptomatic MM, seen at the Royal Adelaide Hospital and Mater Adult Hospital, Brisbane. Aspirates of bone marrow were isolated from posterior superior iliac spine and bone marrow mononuclear cells (BMMNCs) were recovered by density gradient centrifugation and used fresh or were cryopreserved for use at another time. Ethical approval for this study was obtained from the Royal Adelaide Hospital and Mater Adult Hospital, Brisbane institutional ethics review committees.

**Flow cytometry**

Flow cytometry was performed on an LSR II (BD Biosciences, San Jose, CA, USA). GW4869-specific fluorescence was detected using a 405 nm excitation filter and 450/50 nm emission filter (GW4869 spectra shown in Figure S1). For PS staining of cell lines, cells were stained with anti-PS mAb (clone 1H6; Merck Millipore, Bayswater, VIC, Australia) or IgG2a isotype control (clone UPC10; Sigma-Aldrich, Castle Hill, NSW, Australia) followed by anti-mouse IgG AlexaFluor 488 or 647 (Thermo Fisher Scientific, Scoresby, VIC, Australia). For primary MM samples, cell surface PS was assessed on $CD38^{++}$/$CD138^{+}$ plasma cells by multicolour flow cytometry using anti-PS mAb or IgG2a isotype control followed by anti-mouse IgG2a fluorescein isothiocyanate (FITC; Southern Biotech, Birmingham, AL, USA), CD38-PECy7 (HIT2; BioLegend, San Diego, CA, USA) and CD138-AlexaFluor 647 (B-B4; Bio-Rad, Raleigh, NC, USA) mAbs. Data was assessed using FCS Express (De Novo Software, Glendale, CA, USA).

**Cytotoxicity assays**

Cells were incubated with serial dilutions of GW4869 or dimethyl sulphoxide (DMSO) under normal tissue culture conditions. At 72 h, cells were harvested and then stained with propidium iodide and assessed for viability by flow cytometry. It should be noted that GW4869 is excited at violet and UV wavelengths (GW4869 spectra shown in Figure S1),

however this does not interfere with the channel used to detect dead cells which uses a 488 nm laser (Figure S2). For the *in vitro* treatment of BMMNCs from MM patients, samples were treated with the indicated concentrations of GW4869 or vehicle (DMSO). At 24 h, cells were harvested and then stained with anti-CD138 FITC (clone MI15; BD Biosciences) and 7-aminoactinomycin D to exclude dead cells. The proportion of $CD138^+$ cells relative to non-$CD138^+$ cells was determined by flow cytometry. For detection of active caspase 3/7, RPMI-8226 or OPM2 cells were incubated with 5 μM GW4869 or equivalent DMSO control. At 8 h and 24 h, cells were harvested and stained with a Vybrant® caspase 3 and 7 assay kit (Thermo Fisher Scientific). Cells were then assessed by flow cytometry to calculate the proportion of viable, dead and caspase $3/7^+$ cells in the samples.

**$CD122^+$-depleted NOD/SCID MM mouse model**

All experimental work involving animals was approved by the University of Queensland and QIMR Berghofer Medical Research Institute Animal Ethics Committees. Our work was compliant with the approved protocols as well as guidelines set out by the National Health and Medical Research Council (Australia). $CD122^+$-depleted NOD/SCID MM-bearing mice were produced in-house using established protocols (Freeman, *et al* 2011, Sanchez, *et al* 2013). Successful engraftment of green fluorescent protein (GFP)-expressing RPMI-8226 cells was confirmed through the detection of human serum lambda light chain with an enzyme-linked immunosorbent assay (ELISA) (Bethyl Laboratories, Montgomery, TX, USA). Two weeks after engraftment, mice were treated with 1.25 μg/g GW4869 or 2.5% DMSO (vehicle) in 200 μl phosphate-buffered saline (PBS) per day. After 14 days of treatment, mice were humanely killed and serum lambda light chain levels determined by ELISA. In addition, the proportion of bone marrow GFP-expressing RPMI-8226 cells in tibiae, femora and lumbar vertebrae was determined by flow cytometry. The sample sizes chosen for the assessment of serum lambda light chain levels as well as the degree of RPMI-8226 bone marrow engraftment were based on previous experiences with this model (Freeman, *et al* 2011, Sanchez, *et al* 2013). The effects of GW4869 on long-term survival was assessed by treating mice daily until mice either succumbed to disease or were humanely killed due to the acquisition of hind limb paralysis or culled at the end (Day 60) of the experiment. The sample size was estimated using a log-rank sample size estimate (Lachin and Foulkes 1986) based on our previous experiences with this model. We assumed that all mice in the control group would be dead with a treated group showing 35% survival with power of

0.8 and the probability of a type I error of 5%. Moreover, to minimise subjective bias, mice were randomly allocated to the control and treatment group, were kept in the same room in isolated cages, and the studies were performed blinded (an investigator gave the mice a treatment that was not known to them at the time of administration). The ability of GW4869 to incorporate into MM cells *in vivo* was assessed after 10 days of treatment of myeloma-bearing mice with 1.25 µg/g GW4869 or 2.5% DMSO (vehicle) in 200 µl PBS per day. Bone marrow cells were harvested and $GFP^+$ RPMI-8226 myeloma cells were assessed for GW4869-specific fluorescence by flow cytometry. For PS expression on $GFP^+$ RPMI-8226 myeloma cells, bone marrow cells were stained with anti-PS mAb or IgG2a isotype control followed by anti-mouse IgG AlexaFluor 647 and then assessed by flow cytometry.

**Assessment of nSMase2 expression**

For Western blot detection of nSMase2, cells were washed and then lysed with radioimmunoprecipitation assay (RIPA) buffer in the presence of Pierce Protease Inhibitors (Thermo Fisher Scientific). Cell lysates were then separated by reducing sodium dodecyl sulphate polyacrylamide gel electrophoresis (SDS-PAGE) and transferred to a nitrocellulose membrane. The membrane was probed with rabbit anti-nSMase2 (Abcam, Cambridge, UK) followed by anti-rabbit IgG horseradish peroxidase (Sigma-Aldrich) and then assessed by chemiluminescence. ImageJ (https://imagej.nih.gov/ij/) was used to calculate density for the shRNA experiment. For real-time polymerase chain reaction (qPCR) determination of *SMPD3* mRNA expression, total RNA was purified from cells using an RNeasy Plus Mini Kit (Qiagen, Hilden, Germany) and then synthesised into cDNA using Superscript III reverse transcriptase (Thermo Fisher Scientific). cDNA was amplified using SYBR Green qPCR SuperMix with primer pairs specific for *SMPD3* (5‘-ACTTTGATAACTGCTCCTCTGAC-3‘ and 5‘-TTCGTGTCCAGCAGAGTACC-3‘) and the reference gene *RPL36AL* (5‘-GTTAGGCGAGAGCTGCGAAAGG-3‘ and 5‘-GGTTCTTCGGGTTTTAGGTACGTT-3‘). Gene amplification was performed on a Mastercycler EP realplex (Eppendorf, Hamburg, Germany), and relative expression levels were calculated by using the $2^{-\Delta\Delta Ct}$ method (Livak and Schmittgen 2001).

**Sphingomyelin and ceramide quantification**

Lipid extraction was performed according to the method of Matyash *et al* (2008). In brief, 2.5 $\times$ $10^5$ cells, suspended in methanol, were added to a 2.0 ml glass vial containing 750 µl

methyl *tert*-butyl ether, 200 µl methanol and 10 µl internal standard mix(ceramide 17:0 and dihydrosphingomyelin 12:0, both at 20 µM concentration). In order to improve detection of sphingomyelin, hydrolysis of fatty acyl esters was induced by addition of a mild base (Le Lay, *et al* 2009). Sodium hydroxide was added to a final concentration of 0.7 M (75 µl of 10 M). Vials were rotated overnight at 4 $^{o}$C. Ammonium acetate (200 µl of 150 mM) was added and the tubes were vortexed for 30 s and centrifuged at 2000 *g* for 5 min to induce phase separation. The upper organic layer was removed to a new 2 ml glass vial, and stored at -20 $^{o}$C until analysis. Extracts were diluted 5-fold into methanol:chloroform (2:1 v/v) containing 5 mM ammonium acetate prior to mass spectrometric analysis.

Mass spectra were acquired using a chip-based nano-electrospray ionization source (TriVersa Nanomate®, Advion, Ithaca, NY, USA) coupled to a hybrid linear ion trap-triple quadrupole mass spectrometer (QTRAP® 5500, SCIEX, Framingham, MA, USA) as described previously (Montgomery, *et al* 2016). In brief, 10 µl of extract was aspirated from a sealed 96-well plate (Eppendorf Twin-Tec) and delivered into the mass spectrometer via a nano-electrospray ionization (ESI) chip with an orifice diameter of 4.1 µm. The delivery gas was $N_2$ at a pressure of 0.4 psi and a spray voltage of 1.2 kV was used for positive ion. The *m/z* 184.1 precursor ion scan detected choline containing species (sphingomyelins) and the *m/z* 264.4 precursor ion scan detected d18:1 sphingoid-backbone ceramide species. Experimental conditions were a declustering potential of 100 V, entrance potential of 10 V and a scan rate of 200 Da/s. Data were analysed with LipidView® software (SCIEX), including smoothing, identification, removal of isotope contribution from lower mass species and correction for isotope distribution. Quantification was achieved in LipidView® software by comparison of the peak area of individual lipids to their class-specific internal standards after isotope correction.

**shRNA lentiviral knockdown of nSMase2**

Predesigned pGFP-C-shLenti plasmids encoding 4 unique shRNA targeting human *SMPD3* (nSMase2), as well as a scrambled shRNA control, were purchased from OriGene (Rockville, MD, USA; catalogue number TL301492). For expression of lentiviral shRNA constructs in 293T cells, 11 µg of the pGFP-C-shLenti shRNA constructs were co-transfected with 5.5 µg of VSV-G/pMD2.G and 8.25 µg pCMV-dR8.91 using FuGENE6 transfection reagent

(Promega, Madison, WI, USA) in a 10 cm plate. The media was then replaced 4 h later, and then the virus-containing media was harvested at 24 and 48 h, and stored at -80 $^{o}$C until use.

For lentiviral transduction and stable expression of shRNAs, $1 \times 10^6$ RPMI-8226 cells were transferred to 6-well plates pre-coated with recombinant human retronectin fragment (TaKaRa, Mountain View, CA, USA) in 250 μl fresh media containing polybrene (final concentration of 8 μg/ml after addition of lentiviral medium). Lentiviral medium (1 ml) was added to the cells, and the plate was centrifuged at 800 *g* for 30 min and then transferred to an incubator. After 2 h, 2 ml of fresh media was added, and the cells were then subcultured as required over the subsequent days. At day 4, cells were assessed for transduction efficiency by flow cytometry analysing for GFP expression. Cells were then sorted by flow cytometry into a pure $GFP^+$ population with stable expression of the shRNAs. Taqman probes against *SMPD3* (Hs00920354_m1) and *GAPDH* (402869; Thermo Fisher Scientific) were used to assess gene knockdown by qPCR. The pGFP-C-shLenti construct TL301492C showed the lowest expression of *SMPD3*/nSMase2 relative to the scrambled control, which was subsequently used in all knockdown experiments.

**Survival/growth competition assay**

The competition assay was an adaption of a previously described protocol (Jiang, *et al* 2009). Briefly, RPMI-8226 cells were transduced with shRNA targeting *SMPD3*/nSMase2 or a scrambled control. At 72 h after transduction, a sample was taken and assessed by flow cytometry to measure the proportion of shRNA-expressing $GFP^+$ cells to $GFP^-$ non-shRNA-expressing cells. The ratio of $GFP^+$ to $GFP^-$ cells was calculated and normalised to 1, then every subsequent 24 h, cells were assessed to monitor for changes in the proportion of $GFP^+$ to $GFP^-$ cells over time relative to the samples at 72 h.

**Fluorescence microscopy**

The staining reagents used in this study were anti-CD138 FITC (clone MI15) and anti-CD120b biotin (clone hTNFR-M1) from BD Biosciences, anti-mouse IgG AlexaFluor 488 (catologue number A-11001) and streptavidin AlexaFluor 488 (catologue number S-11223), from Thermo Fisher Scientific. In some experiments, cells were pretreated with 5 μM GW4869 for 8 h before staining. For surface staining, cells were stained on ice, washed with 1% bovine serum albumin (BSA) PBS, coated onto poly-L-lysine slides and then fixed in 4%

paraformaldehyde before analysis by confocal microscopy. For intracellular staining, cells were coated onto poly-L-lysine slides, fixed and then permeabilised with 100 μM digitonin for 10 min. Cells were then washed with PBS 1% BSA 0.1% Tween and stained with primary and secondary antibodies. Images were acquired on a Nikon A1 confocal microscope and analysed using NIS-Elements (Nikon, Tokyo, Japan).

**Fluorescence recovery after photobleaching (FRAP) experiments**

OPM2 and RPMI-8226 cells were stained with the cell membrane dye DiI (Thermo Fisher Scientific) and then treated with GW4869 or DMSO control for 4 h under normal tissue culture conditions. Cells were then loaded onto poly-L-lysine coated slides and allowed to rest for 10 min at 37 $^{o}$C. The samples were then analysed on a Nikon A1 confocal microscope using a 100X objective. FRAP experiments were established in three phases using time-lapse data acquisition (500 ms per frame). Phase 1 was the pre-bleach acquisition at an arbitrary laser intensity of 3 (laser 561 nm). Images were recorded over 3 s. Phase 2 was the bleaching acquisition with laser intensity raised to 100 for 8 s. Phase 3 was the post-bleach acquisition at a laser intensity of 3. Post-bleach images were taken over a period of 40 s to allow for fluorescence recovery of the cell membrane. The time-lapses images were then analysed by NIS-Elements software (Nikon). Three regions of interest (ROIs) were used to generate arbitrary fluorescence units over time. ROI 1 measured fluorescence of the bleached region of the cell membrane, ROI 2 measured background fluorescence and ROI 3 measured an unbleached region of the cell membrane. ROIs were then entered into the program easyFRAP using full scale normalisation with a double exponential fitting equation to calculate t-half life and the mobile fraction for each set of images (Rapsomaniki, *et al* 2012).

**GW4869 phospholipid binding studies**

The phospholipids egg phosphatidic acid (PA), 1,2-dioleoyl-*sn*-glycero-3-phosphatidylcholine (PC), 1-palmitoyl-2-oleoyl-*sn*-glycero-3-phosphatidylethanolamine (PE), egg phosphatidylglycerol (PG), soy phosphatidylinositol (PI), 1-palmitoyl-2-oleoyl-*sn*-glycero-3-phosphatidylserine (PS) and egg sphingomyelin were purchased from Avanti Polar Lipids (Alabaster, AL, USA), while soy phosphatidylinositol (PI) was purchased from Sigma-Aldrich. The immobilised binding study was an adaption of previous studies performed in our laboratory (Hutchinson, *et al* 2013, Hutchinson, *et al* 2010). Briefly, phospholipids were dissolved in ethanol (EtOH) and coated onto hydrophobic PolySorp 96-

well plates and $N_2$-dried overnight. Plates were then blocked with 1% BSA PBS for 1 h followed by incubation with 10 μM GW4869 or DMSO vehicle control for 3 h at 37 $^{o}$C. After three washes with 0.3% BSA PBS, the plates were then read on an Infinite 200 plate reader (Tecan, Männedorf, Switzerland) measuring GW4869 fluorescence at excitation and emission wavelengths of 368 nm and 492 nm, respectively.

To test binding of GW4869 to liposomes, mixtures of lipids were dissolved in chloroform then rotary evaporated to deposit a thin film of dried lipid on the glass bulb. Lipids were then freeze-dried overnight and resuspended in PBS at a concentration of 2.5 mg/ml followed by extrusion through 100 nm filters (Hutchinson, *et al* 2013, Hutchinson, *et al* 2010). GW4869 was then added to the liposome mixture at a final concentration of 10 μM in an 850 μl volume and incubated for 2 h at 37 $^{o}$C. The samples were washed twice with 12 ml PBS with liposomes pelleted by ultracentrifugation at 120,000 *g*. The bottom 1 ml (liposome) fraction was then collected and GW4869-specific fluorescence measured at excitation and emission of 368 nm and 492 nm, respectively.

**Brefeldin A (BFA) treatment of MM cells**

MM cells were treated with 2 μg/ml BFA (Sigma-Aldrich) or EtOH vehicle for 4 h. Cells were then harvested and immediately stained for PS or treated with 5 μM GW4869 (or DMSO vehicle) for 12 h to measure uptake of GW4869 by flow cytometry. Samples were also assessed for cell viability by propidium iodide staining, as described above.

**Statistical analysis**

Statistics were performed using GraphPad Prism 6 (GraphPad Software Inc., La Jolla, CA, USA), and the tests used are indicated in the corresponding figure legends. On that note, t-tests were used when the data was assumed to be normally distributed, and Mann Whitney tests were used for to assess the levels of $GFP^+$ RPMI-8226 cell engraftment and serum light chain because the data did not pass the D'Agostino and Pearson omnibus normality test. The variance was not compared between each group of data analysed. A P value of $< 0.05$ was used to define statistical significance.

**RESULTS**

**GW4869 is cytotoxic to MM cells**

During a screen for small molecule anti-MM compounds, we discovered that the small molecule GW4869 (Clarke and Hannun 2006, Marchesini, *et al* 2003; see Figure S3 for chemical structure) was cytotoxic to a panel of MM cell lines but not to non-MM cell lines or PBMCs. All MM cell lines in this panel were sensitive to GW4869, with the exception of U266, which was largely resistant (Figure 1A, B). For some MM cell lines, such as OPM2, cell death was rapid, as a large proportion of dead cells as well as caspase $3/7^+$ cells could be detected as early as 8 h after treatment (Figure 1C). Subsequently, we expanded the number of MM cell lines and non-MM cells used in our cytotoxicity panel to 12 MM cell lines and 8 non-MM cell types, in order to determine if particular genotypes or cell types were more susceptible to GW4869 than others (Table I, Table S1). Six of 12 MM cell lines and 1 of 8 non-MM cell types were found to show some level of sensitivity to GW4869. Classification of MM cell lines based on their translocations and expression of oncogenes did not find any association between genetic abnormalities and GW4869 sensitivity. To confirm that GW4869 was also cytotoxic to primary MM cells, we cultured BMMNCs from MM patients with various concentrations of GW4869 or DMSO vehicle control for 24 h. In 2/3 samples, we observed that GW4869 at 0.4-2.0 μM reduced the proportion of $CD138^+$ MM cells within primary cell cultures (representative shown in Figure 2), suggesting specific cytotoxicity of GW4869 to $CD138^+$ MM cells.

**GW4869 delays MM tumour growth in a xenograft model**

We next set out to determine whether GW4869 could suppress the growth of a MM cell line *in vivo*. In these experiments we used an established MM xenograft model that replicates human disease, with growth of MM cells within the bone marrow (Freeman, *et al* 2011, Sanchez, *et al* 2013). Briefly, GFP-expressing RPMI-8226 cells were injected i.v. into γ-irradiated, $CD122^+$-depleted NOD/SCID mice. At day 9, mice that were successfully engrafted (determined by detection of human lambda light chain in serum) were treated daily with i.p. injections of 1.25 μg/g GW4869 or DMSO vehicle control. After two weeks of treatment, mice were humanely killed and serum lambda light chain levels and the proportion of $GFP^+$ RPMI-8226 cells in bone marrow aspirates were assessed. The GW4869-treated group showed reduced levels of lambda light chain (mean: 0.7 *vs.* 1.9 μg/ml for GW4869 and vehicle, respectively; Figure 3A). There was also a decrease in $GFP^+$ RPMI-8226 cells in the GW4869-treated group in the femur/tibia as well as the lumbar spine which was not

significant (Figure 3B); however, when both tissues were combined, GW4869-treated mice showed a significant decrease in the levels of $GFP^+$ RPMI-8226 cells relative to the vehicle control (Figure 3C). Finally, we performed a long-term survival experiment where mice were treated daily with GW4869 or vehicle. The GW4869-treated group survived longer than the vehicle control-treated group with the median survival time of 38 and 28 days, respectively (hazard ratio: 2.61, 95% confidence interval: 1.13-9.07; Figure 3D). These findings confirm that GW4869 is capable of suppressing MM growth *in vivo*.

**nSMase2 expression does not correlate with sensitivity to GW4869**

In order to understand the mechanism by which GW4869 is cytotoxic to MM cells, we initially tested the expression of its presumed target, nSMase2 (Clarke and Hannun 2006, Marchesini, *et al* 2003, Shamseddine, *et al* 2015), in MM cell lines and in GW4869-resistant non-MM cells. nSMase2 and its gene (*SMPD3*) were detected in all cell lines by Western blot and qPCR, respectively (Figure 4A, B). However, there was no association between nSMase2 expression and sensitivity to GW4869 as one of the most GW4869-sensitive cell lines, OPM2, had close to undetectable levels of nSMase2. Furthermore, two GW4869-resistant non-MM cell lines, Jurkat and K562, displayed similar levels of nSMase2 to the GW4869-sensitive MM cell lines NCI-H929 and JJN3.

To ascertain whether GW4869 suppresses the turnover of sphingomyelin to ceramide, and thus inhibits nSMase2 in MM cells, we treated RPMI-8226 and OPM2 cells with GW4869 for 4, 9 and 24 h and then measured total sphingomyelin and ceramide species by ESI-MS. In contrast to the expected effects of nSMase2 inhibition, the molar levels of sphingomyelin decreased while ceramide increased in treated cells suggesting that GW4869 is not inhibiting nSMase2 in MM cells (Figure 4C). We then used a shRNA specific for *SMPD3* (the gene that encodes nSMase2) and delivered by a GFP-expressing lentiviral vector, to knockdown the expression of the enzyme in GW4869 sensitive RPMI-8226 cells. We achieved a knockdown of *SMPD3*/nSMase2 expression of approximately 4-fold at the mRNA level (23.5% of the scrambled control Figure 5A), however there was only a modest, but not convincing knockdown of nSMase2 by Western blot (~20% knockdown of nSMase2 compared to control; Figure 5B). Nevertheless, we then assessed the effects of *SMPD3* shRNA knockdown on cellular survival and proliferation by using a competition assay. This assay measures the relative abundance of $GFP^+$ shRNA-expressing cells in a partially transduced population over time. $GFP^+$ cells that express an shRNA that confers a survival disadvantage

and/or inhibits proliferation will be outgrown by the non-transduced $GFP^-$ cells (Jiang, *et al* 2009). We found that the $GFP^+$ transduced cells grew at the same rate as $GFP^-$ non-transduced cells for both the scrambled and *SMPD3* shRNA samples (Figure 5C). This suggests that reduced *SMPD3* mRNA expression has no effect on RPMI-8226 cell survival/proliferation. Finally, we tested the ability of GW4869 to induce cytotoxicity in RPMI-8226 cells with reduced *SMPD3* mRNA expression. We found that there was no difference in the amount of cell death between the scrambled and *SMPD3* shRNA-expressing cells. Given that nSMase2 protein levels were not convincingly knocked down by *SMPD3* shRNAs, we cannot conclude with confidence that the cytotoxic effects of GW4869 on MM cells is independent of nSMase2 inhibition. However, when combined with the fact that GW4869 does not inhibit the turnover of sphingomyelin to ceramide in these cells, as well as there being no correlation between nSMase2 expression and GW4869 sensitivity, there is no evidence to support that the cytotoxic effects of GW4869 is due to direct nSMase2 inhibition.

**GW4869 localizes and deforms the cell membrane of MM cells**

GW4869 shows an excitation and emission peak at 368 nm and 492 nm, respectively (Figure S3, which makes it suitable to use in fluorescence applications. We used these properties of GW4869 to define its subcellular localisation in MM cells, and found that GW4869 co-localised with the cell membrane markers CD138 and CD120b on RPMI-8226 cells (Figure 6). Importantly, there was no bleed through of GW4869-specific fluorescence into the green channel (Figure S4). Another observation was that the cell membranes of these GW4869-treated cells were grossly deformed and ruffled, with both CD138 and CD120b clustered alongside GW4869 in the same region of the cell. This was in contrast to vehicle control-treated cells where both CD138 and CD120b were more uniformly distributed around the cell membrane (Figure 6). These results suggest that GW4869 interacts with a component of the cell membrane and causes distortions in regions where it accumulates.

In order to assess other morphological changes in the cell membrane of GW4869-treated MM cells, we performed FRAP experiments to measure the effects of the compound on cell membrane fluidity, which is a critical aspect of cellular function (Nicolson 2014). GW4869-treated OPM2 cells were found to have significantly reduced membrane fluidity relative to vehicle-treated cells, with a mean half-life of 4.87 s versus 2.67 s for DMSO (Table II). Furthermore, the mobile fraction, a measure of how many molecules are in a fluid state as opposed to solid state in the cell membrane (1.0 being all molecules fluid and 0.0 being no

molecules fluid), had a mean value of 0.91 for DMSO-treated cells versus 0.64 for GW4869-treated cells (Table II, Figure 7). Similar results were also observed with RPMI-8226 cells (mean t-half-life of 4.40 s and 7.10 s, and mean mobile fraction of 0.85 and 0.69 for DMSO and GW4869, respectively; Table II). This data clearly shows that GW4869 rigidifies the cell membrane of MM cells and provides further evidence that this compound induces gross cell membrane deformities.

**GW4869 binds to anionic phospholipids**

The fact that GW4869 localises to the cell membrane of MM cells as well as being very hydrophobic suggested that the molecule might bind directly to the bilayer through associating with cell membrane lipids. To test this hypothesis, we assessed the ability of GW4869 to interact with different classes of phospholipid species immobilised onto 96-well hydrophobic plates. Interestingly, GW4869 showed high levels of binding to the anionic phospholipids PS, PA and PG. In contrast, little to no binding of GW4869 was observed for sphingomyelin, PC, PE and PI (Figure 8A). To confirm that GW4869 interacts with anionic phospholipids, we synthesised liposomes composed of different ratios of anionic to zwitterionic lipid species. In this assay, the zwitterionic phospholipid PC was used as the base lipid as this forms stable liposomes. PC was used alone or mixed in a 3:1 ratio with the anionic phospholipids PS or PA. Liposomes were then incubated with 10 μM GW4869 for 2 h and washed extensively to remove unbound GW4869. The liposome fraction was then assessed for GW4869 uptake by measuring direct fluorescence of the compound. GW4869 bound strongly to PS/PC and PA/PC liposomes and showed low levels of binding to PC only liposomes, which confirmed that GW4869 preferentially binds to anionic phospholipids (Figure 8B).

**MM cells express surface exposed PS**

The fact that GW4869 binds to anionic phospholipids as well as being incorporated into the membrane of MM cells suggests that the cytotoxic effects of the compound may be due to the presence of cell surface anionic phospholipids. In order to investigate this, we initially tested the ability for GW4869 to be taken up into the cell membranes of GW4869-sensitive MM cells and GW4869-resistant non-MM cells. Cells were treated for 4 h with 5 μM GW4869 and then assessed by flow cytometry to assess GW4869-specific fluorescence. Interestingly, the MM cells incorporated high levels of GW4869 into their cell membranes with U266 cells,

which are resistant to GW4869, showing the least amount of uptake. In contrast, the non-MM cells showed only low levels of GW4869 uptake (Figure 9A, B, C). We also assessed the ability of GW4869 to be incorporated into MM cells *in vivo*. After 10 days of treatment, approximately 25% of bone marrow $GFP^+$ RPMI-8226 cells had taken up GW4869, thus confirming that the small cationic molecule can interact with MM cells *in vivo* (Figure 9D). As GW4869 bound strongly to PS, the major anionic phospholipid found in eukaryotic cell membranes (Leventis and Grinstein 2010), we stained MM cell lines and non-MM cells with an anti-PS mAb to determine if sensitivity to GW4869 by MM cells could result from the presence of anionic phospholipids on the cell surface. All MM cell lines tested were found to express cell surface PS, with 6/12 MM cell lines expressing high levels of cell surface PS (Table I). In addition, RPMI-8226 cells engrafted into the bone marrow of $CD122^+$-depleted NOD/SCID mice were also found to express high levels of surface PS (Figure 10A). In contrast, PBMCs and the majority of non-MM cell lines tested did not express cell surface PS (Figure 10B, Table S1). The sensitivity of cells to GW4869 correlated closely with PS expression. For example, 5 out of the 6 high PS expressing cell lines were sensitive to GW4869, and for the moderate PS expressing cell lines, 2/5 were sensitive (this includes the B-ALL cell line, Nalm-6). In contrast, all cell types with either low or no PS expression were found to be resistant to GW4869 (Table I, Table S1). Therefore, these results show that the levels of PS expression correlate well with sensitivity to GW4869.

Extracellular exposure of PS is normally synonymous with dead or dying cells, such as in apoptosis. However, MM cell lines were not found to be apoptotic, as they: 1) did not show any increase in basal caspase $3/7^+$ activity over non-MM cell lines (Figure S5), and 2) induction of apoptosis using mitomycin C induced a two order of magnitude increase in cell surface PS compared with untreated MM cells (Figure 10C).

Given that extracellular PS was expressed on MM cell lines, we also stained MM $CD138^+$ primary cells to ascertain whether they also expose PS. Nine out of 15 samples showed some level of externalised PS on $CD38^+/CD138^+$ MM plasma cells. Of these PS positive samples, five were found to express moderate to high levels of PS with the other four having detectable but low levels on the surface (Figure 10D, E; Table S2). Two of the three primary patient samples tested for GW4869-specific cytotoxicity (Figure 2, above) were also assessed for cell surface PS expression. Interesting, the GW4869-resistant patient was a non-PS

expressor, whereas the GW4869-sensitive patient tested was found to express high levels of cell surface PS (Patient 3 and Patient 15, respectively).

**Secretion is responsible for PS exposure on MM cells**

It has been found that excited neuronal cells and activated mast cells can "flip-out" PS onto the extracellular face, which is thought to be as a result of the fusion of intracellular compartments, such as secretory vesicles, with the cell membrane (Leventis and Grinstein 2010, Ory, *et al* 2013). Given that MM cells are highly secretory due to synthesis of immunoglobulin, we set out to determine whether PS exposure is related to secretion in these cells. MM cell lines were treated with the well-known secretion inhibitor BFA or vehicle control for 4 h and then stained for PS as before. All cell lines were found to down regulate the levels of PS on their surface by approximately 25 to 50% with BFA treatment, suggesting that secretion is at least partly responsible for this phenomenon (Figure 11A). We then incubated the same cells with GW4869 for 12 h and found that BFA-treated samples accumulated 50-75% lower amounts of GW4869 compared with vehicle control-treated cells (Figure 11A). In addition to this, we also assessed the ability for BFA to inhibit GW4869-specific cytotoxicity. As BFA is cytotoxic within 24–48 h, we conducted our experiment over a shorter time period (16 h total). RPMI-8226 cells and OPM2 cells were pre-treated with BFA or EtOH vehicle control for 4 h followed by incubation with GW4869 or DMSO vehicle control for 12 h before assessment of cell viability. As expected, cells pre-treated with EtOH vehicle control were susceptible to GW4869 with approximately 25% more cytotoxicity than DMSO for both cell lines. However, there was no difference in viability between DMSO and GW4869 for the BFA pre-treated samples (Figure 11B). Given that BFA-treated cells became resistant to the effects of GW4869, our results suggest that PS exposure and subsequent cytotoxicity to GW4869 may be attributed to secretion by MM cells.

**DISCUSSION**

We demonstrate that a large proportion of MM cells and cell lines express exoplasmic PS. Moreover, targeting PS with a small cationic molecule can induce cytotoxicity in high surface PS-expressing MM cells and inhibit the growth of MM cells *in vivo*. PS is normally confined to the intracellular side of the cell membrane in healthy cells through an active process that is regulated by the activity of ATP-driven flippases. It is well-known that dead or dying cells

lose the ability to regulate cell membrane asymmetry resulting in the exoplasmic expression of PS (Leventis and Grinstein 2010). However in our studies, cell surface PS-expressing MM cells were not found to be apoptotic. Cell surface PS has also been described for other cell types, such as activated platelets, mast cells and neuronal cells (Leventis and Grinstein 2010, Ory, *et al* 2013). Additionally, it has also been shown that a number of cancer types, including glioblastoma and melanoma, as well as endothelial cells in tumour vasculature can express exoplasmic PS (DeRose, *et al* 2011, Riedl, *et al* 2011). The mechanisms that induce PS exposure on the surface of these cells are not well understood. One theory posits that activated cells increase cytoplasmic $Ca^{2+}$ levels which, in turn, activate scramblases, leading to PS translocation to the cell surface (Riedl, *et al* 2011). It has also been proposed that exocytosis of secretory vesicles can lead to the transient exposure of PS as a consequence of local perturbations from membrane fusion, or the presence of PS on the outer leaflet of secretory vesicle membranes (Martin, *et al* 2000, Zwaal and Schroit 1997). In relation to our studies, we present evidence that at least some of the PS exposure on MM cells may be attributed to secretion. Indeed, MM cells are considered a secretory cell given that they synthesise and secrete large amounts of immunoglobulin. Therefore PS exposure may be a general property of cells actively involved in secretion.

The small cationic molecule GW4869 is the most commonly used inhibitor of nSMase2 in cell-based assays (Shamseddine, *et al* 2015). In our studies, we did not find evidence that the cytotoxic effects of GW4869 in MM cells could be attributed to inhibition of nSMase2. For example, cells of the OPM2 cell line, which is one of the most sensitive cell lines to GW4869, showed low to undetectable levels of nSMase2 expression. Furthermore, the ratio of sphingomyelin to ceramide remains unchanged or actually decreases in GW4869-treated MM cell lines, which is in contrast to the expected effects of nSMase2 inhibition. Unfortunately, we were unable to definitely rule out nSMase2 in the cytotoxic pathway as specific knockdown with shRNAs only resulted in a modest and unconvincing knockdown at the protein level (despite *SMPD3* mRNA levels being ~25% of control). Therefore subsequent studies may need to use more effective knockdown strategies, such as the use of Clustered regularly interspaced short palindromic repeats (CRISPR)/Cas9 to disrupt expression all together and confirm that GW4869-induced cytotoxicity is independent of nSMase2.

Our results suggest sensitivity to GW4869 is dependent upon surface expression of PS. This was based on the observation that GW4869 binds to anionic phospholipids, such as PS, that the levels of surface PS expression are well correlated with sensitivity to GW4869, and that reduction in exoplasmic PS levels using BFA causes a lower uptake of GW4869 and reduced cytotoxicity of the compound. Interestingly, PS is a co-factor for nSMase2 activity (Marchesini, *et al* 2003, Shamseddine, *et al* 2015). Therefore, the GW4869 inhibition of nSMase2 observed in other studies may occur indirectly, through binding and sequestration of PS. Nevertheless, the fact that GW4869 binds to anionic phospholipids suggests that the inhibitor is not as specific to nSMase2 as previously thought. Results using GW4869 should be interpreted with caution unless supported by other inhibitors, such as siRNAs or targeted gene disruption complexes, confirming that phenotypic changes are due to inhibition of nSMase2 and not through interaction with anionic phospholipids. On that note, we have reported phenotypic changes in MM cells treated with GW4869 in a prior study (Hutchinson, *et al* 2010). This was assumed to be due to nSMase2 inhibition; however, the end point of these experiments was at 48 h, a time that the many of these cells are dead or dying. Thus it is possible that phenotypic changes were due to cytotoxic effects of the compound targeting cell surface PS rather than through nSMase2 inhibition (Hutchinson, *et al* 2010). GW4869 is also frequently used as an inhibitor of exosome secretion, which is attributed to nSMase2 inhibition (Colombo, *et al* 2014). However, exosomes display PS on both sides of the membrane (Matsumoto, *et al* 2017). Therefore inhibition of exosome secretion by GW4869 may be due to binding to PS on the exosome membrane rather than through nSMase2 inhibition, which should be explored in subsequent studies.

There are a number of possible mechanisms to explain the cytotoxic effects induced by GW4869 binding to PS. GW4869 was found to grossly deform the cell membrane, which led to significant changes in fluidity as well as clustering of integral membrane proteins. The regulation of cell membrane fluidity is an essential aspect of cellular function (Nicolson 2014), and the rigidifying effects of GW4869 may have disrupted critical pathways, such as the transportation of nutrients or disruption of cell signalling, which are required for cell survival. On the other hand, the clustering of integral membrane proteins, which was also observed in our study, can lead to aberrant cell signalling and subsequent cell death (Gajate and Mollinedo 2007, Sessler, *et al* 2013). That said, caspase 8 is a known inducer of the extrinsic (cell membrane) apoptotic pathway (Lavrik, *et al* 2005, Sessler, *et al* 2013). However, we found no evidence of caspase 8 activation, nor were we able to block

cytotoxicity using a specific inhibitor of caspase 8 (Figure S6). We also assessed caspase 9 activation to see if there is any evidence that the intrinsic apoptosis pathway is activated, however similar to caspase 8, there was no detectable increase in caspase 9 activity (Figure S7). Alternatively, GW4869 may disrupt cell membrane integrity. For example, the compound is large and highly cationic (predicted p$K_a$ of 9.68), which probably mediates its interaction with anionic phospholipids, and in many ways it resembles a cationic peptide, such as a defensin. Cationic peptides are cytolysins that preferentially interact with anionic membranes (Bankovic, *et al* 2013, Ganz 2003, Liu, *et al* 2016, Schroder-Borm, *et al* 2005). Thus it is possible that GW4869 acts in a similar manner to these peptides by accumulating on the surface of anionic phospholipids and eventually disrupting cell membrane integrity, leading to cell death.

The levels of PS expression are associated with sensitivity to GW4869. For example, 5/6 high PS expressing cell lines are sensitive to GW4869, whereas only 1/4 moderate PS expressing MM cell lines showed susceptibility to GW4869. Thus small molecules targeting PS are likely to be most effective in this high PS expressing subgroup. In relation to MM patients, our results suggest that high cell surface PS expression is a feature of MM plasma cells from a subset of patients (2/15 samples analysed). Furthermore, it appears that MM primary cells with high PS expression are sensitive at relatively low concentrations of GW4869, however dose responses remain to be defined, and it is also not known if primary MM plasma cells expressing moderate levels of PS might be sensitive to GW4869, which will need to be addressed in subsequent studies. Although high levels of PS expression is characteristic of only a small subgroup of MM patients, this is still significant given the current trend towards personalised, MM subtype-specific therapies. For example, the finding that 4% of MM patients express activating mutations in the oncogene *BRAF* (Chapman, *et al* 2011), led to the clinical testing of *BRAF* inhibitors in this subgroup of patients (Hyman, *et al* 2015).

Another avenue to explore is whether surface PS expression is related to the stage of disease, and whether it could be used as a prognostic marker for MM. Although not the purpose of this study, it is interesting to note there does not appear to be any correlation between surface PS expression and the stage of MM (according to the International Scoring System classification). However, of the moderate to high PS expressing samples where there is information on survival, only 1/4 patients were still alive at follow-up as opposed to 6/8 patients with low to no PS expression. This suggests that the levels of PS expression might be

negatively correlated with survival, which could be confirmed using a larger pool of patient samples.

GW4869 is only a "proof of concept" first generation compound and there is probably much room to improve its potency and pharmacokinetics. For example, after a 10-day treatment with GW4869, approximately 25% of RPMI-8226 cells had taken up the compound *in vivo*. This was modest, however it was enough to delay the growth of these cells in this model. Therefore subsequent medicinal chemistry studies should focus on improving the pharmacokinetics and potency of second generation anti-PS compounds to enhance their efficacy *in vivo*, as well as testing them for synergistic effects with other types of therapies, especially those that are already approved for the treatment of MM. Finally, PS targeting small molecules should be assessed on other types of cancers given the fact that the B-ALL cell line, Nalm-6, was found to express PS and was also sensitive to GW4869. This includes PS-expressing cancers, such as glioblastoma and melanoma (Riedl, *et al* 2011, Utsugi, *et al* 1991). Moreover, there are only a small number of studies reporting the surface expression of PS on malignant cells (Bankovic, *et al* 2013, Riedl, *et al* 2011, Schroder-Borm, *et al* 2005), so subsequent studies will be required to determine the PS expression profile on other types of cancers as well as their sensitivity to PS targeting agents.

To the best of our knowledge, this is the first study to demonstrate that a small molecule targeting PS can lead to the selective cytotoxicity of surface PS-expressing malignant cells and inhibiting the growth of MM cells *in vivo*. Moreover, exoplasmic PS has been considered a potential therapeutic target for a variety of other cancers (Bankovic, *et al* 2013, Riedl, *et al* 2011, Schroder-Borm, *et al* 2005). It is also found on the surface of vasculature endothelial cells within solid tumours. This has led to the preclinical and clinical testing of novel PS-targeting molecules, such as cationic peptides and anti-PS mAbs (Bankovic, *et al* 2013, DeRose, *et al* 2011, Schroder-Borm, *et al* 2005); however, a small molecule approach has yet to be assessed. Given the findings of our study, we argue that novel PS targeting small molecules should also be evaluated as an alternative therapeutic strategy for the treatment of surface PS-expressing tumours.

**FUNDING SOURCES**

This work was supported by a Cure Cancer Australia and Cancer Australia Priority Driven grant (#1050067). ATH was a recipient of a Chancellor's Postdoctoral Fellowship at the University of Technology, Sydney and a Fulbright Postdoctoral Fellowship at Yale University. KV was supported by a Mary Overton Early Career Research Fellowship (Royal Adelaide Hospital). GRH is a NHMRC Australia Fellow and QLD Health Senior Clinical Research Fellow.

**ACKNOWLEDGEMENTS**

The authors gratefully acknowledge the contribution toward this study from the Victorian Operational Infrastructure Support Program received by the Burnet Institute.

**AUTHOR CONTRIBUTIONS**

ATH designed the study, performed experiments, analysed data and wrote the paper. SV, KV, SHJB, TWM performed experiments, analysed data and contributed to writing the paper. DAR and PMW performed experiments and analysed data. EY, BC, JL, JL, PWA and PAR analysed data, provided intellectual input and contributed to writing the paper. GRH and ACWZ provided samples, analysed data, provided intellectual input and contributed writing to the paper.

**CONFLICT OF INTEREST**

The authors declare that there are no conflicts of interest. Note, ATH is currently an employee of Alexion Pharmaceuticals, however, this work was done prior to him joining the company.

**REFERENCES**

Bankovic, J., Andra, J., Todorovic, N., Podolski-Renic, A., Milosevic, Z., Miljkovic, D., Krause, J., Ruzdijic, S., Tanic, N. & Pesic, M. (2013) The elimination of P-glycoprotein over-expressing cancer cells by antimicrobial cationic peptide NK-2: the unique way of multi-drug resistance modulation. *Exp Cell Res,* **319,** 1013-1027.

Chapman, M.A., Lawrence, M.S., Keats, J.J., Cibulskis, K., Sougnez, C., Schinzel, A.C., Harview, C.L., Brunet, J.P., Ahmann, G.J., Adli, M., Anderson, K.C., Ardlie, K.G., Auclair, D., Baker, A., Bergsagel, P.L., Bernstein, B.E., Drier, Y., Fonseca, R., Gabriel, S.B., Hofmeister, C.C.,

Jagannath, S., Jakubowiak, A.J., Krishnan, A., Levy, J., Liefeld, T., Lonial, S., Mahan, S., Mfuko, B., Monti, S., Perkins, L.M., Onofrio, R., Pugh, T.J., Rajkumar, S.V., Ramos, A.H., Siegel, D.S., Sivachenko, A., Stewart, A.K., Trudel, S., Vij, R., Voet, D., Winckler, W., Zimmerman, T., Carpten, J., Trent, J., Hahn, W.C., Garraway, L.A., Meyerson, M., Lander, E.S., Getz, G. & Golub, T.R. (2011) Initial genome sequencing and analysis of multiple myeloma. *Nature,* **471,** 467-472.

Clarke, C.J. & Hannun, Y.A. (2006) Neutral sphingomyelinases and nSMase2: bridging the gaps. *Biochim Biophys Acta,* **1758,** 1893-1901.

Colombo, M., Raposo, G. & Thery, C. (2014) Biogenesis, secretion, and intercellular interactions of exosomes and other extracellular vesicles. *Annu Rev Cell Dev Biol,* **30,** 255-289.

DeRose, P., Thorpe, P.E. & Gerber, D.E. (2011) Development of bavituximab, a vascular targeting agent with immune-modulating properties, for lung cancer treatment. *Immunotherapy,* **3,** 933-944.

Digumarti, R., Bapsy, P.P., Suresh, A.V., Bhattacharyya, G.S., Dasappa, L., Shan, J.S. & Gerber, D.E. (2014) Bavituximab plus paclitaxel and carboplatin for the treatment of advanced non-small-cell lung cancer. *Lung Cancer,* **86,** 231-236.

Dingjan, T., Spendlove, I., Durrant, L.G., Scott, A.M., Yuriev, E. & Ramsland, P.A. (2015) Structural biology of antibody recognition of carbohydrate epitopes and potential uses for targeted cancer immunotherapies. *Mol Immunol,* **67,** 75-88.

Freeman, L.M., Lam, A., Petcu, E., Smith, R., Salajegheh, A., Diamond, P., Zannettino, A., Evdokiou, A., Luff, J., Wong, P.F., Khalil, D., Waterhouse, N., Vari, F., Rice, A.M., Catley, L., Hart, D.N. & Vuckovic, S. (2011) Myeloma-induced alloreactive T cells arising in myeloma-infiltrated bones include double-positive CD8+CD4+ T cells: evidence from myeloma-bearing mouse model. *J Immunol,* **187,** 3987-3996.

Gajate, C. & Mollinedo, F. (2007) Edelfosine and perifosine induce selective apoptosis in multiple myeloma by recruitment of death receptors and downstream signaling molecules into lipid rafts. *Blood,* **109,** 711-719.

Ganz, T. (2003) Defensins: antimicrobial peptides of innate immunity. *Nat Rev Immunol,* **3,** 710-720.

Hutchinson, A.T., Ramsland, P.A., Jones, D.R., Agostino, M., Lund, M.E., Jennings, C.V., Bockhorni, V., Yuriev, E., Edmundson, A.B. & Raison, R.L. (2010) Free Ig light chains interact with sphingomyelin and are found on the surface of myeloma plasma cells in an aggregated form. *J Immunol,* **185,** 4179-4188.

Hutchinson, A.T., Malik, A., Berkahn, M.B., Agostino, M., To, J., Tacchi, J.L., Djordjevic, S.P., Turnbull, L., Whitchurch, C.B., Edmundson, A.B., Jones, D.R., Raison, R.L. & Ramsland, P.A. (2013)

Formation of assemblies on cell membranes by secreted proteins: molecular studies of free lambda light chain aggregates found on the surface of myeloma cells. *Biochem J,* **454,** 479-489.

Hyman, D.M., Puzanov, I., Subbiah, V., Faris, J.E., Chau, I., Blay, J.Y., Wolf, J., Raje, N.S., Diamond, E.L., Hollebecque, A., Gervais, R., Elez-Fernandez, M.E., Italiano, A., Hofheinz, R.D., Hidalgo, M., Chan, E., Schuler, M., Lasserre, S.F., Makrutzki, M., Sirzen, F., Veronese, M.L., Tabernero, J. & Baselga, J. (2015) Vemurafenib in Multiple Nonmelanoma Cancers with BRAF V600 Mutations. *N Engl J Med,* **373,** 726-736.

Jiang, H., Reinhardt, H.C., Bartkova, J., Tommiska, J., Blomqvist, C., Nevanlinna, H., Bartek, J., Yaffe, M.B. & Hemann, M.T. (2009) The combined status of ATM and p53 link tumor development with therapeutic response. *Genes Dev,* **23,** 1895-1909.

Lachin, J.M. & Foulkes, M.A. (1986) Evaluation of sample size and power for analyses of survival with allowance for nonuniform patient entry, losses to follow-up, noncompliance, and stratification. *Biometrics,* **42,** 507-519.

Lavrik, I., Golks, A. & Krammer, P.H. (2005) Death receptor signaling. *J Cell Sci,* **118,** 265-267.

Le Lay, S., Li, Q., Proschogo, N., Rodriguez, M., Gunaratnam, K., Cartland, S., Rentero, C., Jessup, W., Mitchell, T. & Gaus, K. (2009) Caveolin-1-dependent and -independent membrane domains. *J Lipid Res,* **50,** 1609-1620.

Leventis, P.A. & Grinstein, S. (2010) The distribution and function of phosphatidylserine in cellular membranes. *Annu Rev Biophys,* **39,** 407-427.

Liu, X., Cao, R., Wang, S., Jia, J. & Fei, H. (2016) Amphipathicity Determines Different Cytotoxic Mechanisms of Lysine- or Arginine-Rich Cationic Hydrophobic Peptides in Cancer Cells. *J Med Chem,* **59,** 5238-5247.

Livak, K.J. & Schmittgen, T.D. (2001) Analysis of relative gene expression data using real-time quantitative PCR and the 2(-Delta Delta C(T)) Method. *Methods,* **25,** 402-408.

Marchesini, N., Luberto, C. & Hannun, Y.A. (2003) Biochemical properties of mammalian neutral sphingomyelinase 2 and its role in sphingolipid metabolism. *J Biol Chem,* **278,** 13775-13783.

Martin, S., Pombo, I., Poncet, P., David, B., Arock, M. & Blank, U. (2000) Immunologic stimulation of mast cells leads to the reversible exposure of phosphatidylserine in the absence of apoptosis. *Int Arch Allergy Immunol,* **123,** 249-258.

Matsumoto, A., Takahashi, Y., Nishikawa, M., Sano, K., Morishita, M., Charoenviriyakul, C., Saji, H. & Takakura, Y. (2017) Role of Phosphatidylserine-Derived Negative Surface Charges in the Recognition and Uptake of Intravenously Injected B16BL6-Derived Exosomes by Macrophages. *J Pharm Sci,* **106,** 168-175.

Matyash, V., Liebisch, G., Kurzchalia, T.V., Shevchenko, A. & Schwudke, D. (2008) Lipid extraction by methyl-tert-butyl ether for high-throughput lipidomics. *J Lipid Res,* **49,** 1137-1146.

Mollinedo, F. & Gajate, C. (2015) Lipid rafts as major platforms for signaling regulation in cancer. *Adv Biol Regul,* **57,** 130-146.

Montgomery, M.K., Brown, S.H., Lim, X.Y., Fiveash, C.E., Osborne, B., Bentley, N.L., Braude, J.P., Mitchell, T.W., Coster, A.C., Don, A.S., Cooney, G.J., Schmitz-Peiffer, C. & Turner, N. (2016) Regulation of glucose homeostasis and insulin action by ceramide acyl-chain length: A beneficial role for very long-chain sphingolipid species. *Biochim Biophys Acta,* **1861,** 1828-1839.

Moreaux, J., Klein, B., Bataille, R., Descamps, G., Maiga, S., Hose, D., Goldschmidt, H., Jauch, A., Reme, T., Jourdan, M., Amiot, M. & Pellat-Deceunynck, C. (2011) A high-risk signature for patients with multiple myeloma established from the molecular classification of human myeloma cell lines. *Haematologica,* **96,** 574-582.

Nicolson, G.L. (2014) The Fluid-Mosaic Model of Membrane Structure: still relevant to understanding the structure, function and dynamics of biological membranes after more than 40 years. *Biochim Biophys Acta,* **1838,** 1451-1466.

Nitulescu, G.M., Margina, D., Juzenas, P., Peng, Q., Olaru, O.T., Saloustros, E., Fenga, C., Spandidos, D., Libra, M. & Tsatsakis, A.M. (2016) Akt inhibitors in cancer treatment: The long journey from drug discovery to clinical use (Review). *Int J Oncol,* **48,** 869-885.

Ory, S., Ceridono, M., Momboisse, F., Houy, S., Chasserot-Golaz, S., Heintz, D., Calco, V., Haeberle, A.M., Espinoza, F.A., Sims, P.J., Bailly, Y., Bader, M.F. & Gasman, S. (2013) Phospholipid scramblase-1-induced lipid reorganization regulates compensatory endocytosis in neuroendocrine cells. *J Neurosci,* **33,** 3545-3556.

Rapsomaniki, M.A., Kotsantis, P., Symeonidou, I.E., Giakoumakis, N.N., Taraviras, S. & Lygerou, Z. (2012) easyFRAP: an interactive, easy-to-use tool for qualitative and quantitative analysis of FRAP data. *Bioinformatics,* **28,** 1800-1801.

Riedl, S., Rinner, B., Asslaber, M., Schaider, H., Walzer, S., Novak, A., Lohner, K. & Zweytick, D. (2011) In search of a novel target - phosphatidylserine exposed by non-apoptotic tumor cells and metastases of malignancies with poor treatment efficacy. *Biochim Biophys Acta,* **1808,** 2638-2645.

Ronchetti, D., Bogni, S., Finelli, P., Lombardi, L., Otsuki, T., Maiolo, A.T. & Neri, A. (2001) Characterization of the t(4;14)(p16.3;q32) in the KMS-18 multiple myeloma cell line. *Leukemia,* **15,** 864-865.

Sanchez, W.Y., McGee, S.L., Connor, T., Mottram, B., Wilkinson, A., Whitehead, J.P., Vuckovic, S. & Catley, L. (2013) Dichloroacetate inhibits aerobic glycolysis in multiple myeloma cells and increases sensitivity to bortezomib. *Br J Cancer,* **108,** 1624-1633.

Schroder-Borm, H., Bakalova, R. & Andra, J. (2005) The NK-lysin derived peptide NK-2 preferentially kills cancer cells with increased surface levels of negatively charged phosphatidylserine. *FEBS Lett,* **579,** 6128-6134.

Sessler, T., Healy, S., Samali, A. & Szegezdi, E. (2013) Structural determinants of DISC function: new insights into death receptor-mediated apoptosis signalling. *Pharmacol Ther,* **140,** 186-199.

Shamseddine, A.A., Airola, M.V. & Hannun, Y.A. (2015) Roles and regulation of neutral sphingomyelinase-2 in cellular and pathological processes. *Adv Biol Regul,* **57,** 24-41.

Soliman, C., Yuriev, E. & Ramsland, P.A. (2017) Antibody recognition of aberrant glycosylation on the surface of cancer cells. *Curr Opin Struct Biol,* **44,** 1-8.

Teoh, P., Chung, T., Sebastian, S., Choo, S., Yan, J., Ng, S., Fonseca, R. & Chng, W. (2014) p53 Haploinsufficiency and Functional Abnormalities in Multiple Myeloma. *Leukemia*, **28**, 2066-2074

Utsugi, T., Schroit, A.J., Connor, J., Bucana, C.D. & Fidler, I.J. (1991) Elevated expression of phosphatidylserine in the outer membrane leaflet of human tumor cells and recognition by activated human blood monocytes. *Cancer Res,* **51,** 3062-3066.

Zwaal, R.F. & Schroit, A.J. (1997) Pathophysiologic implications of membrane phospholipid asymmetry in blood cells. *Blood,* **89,** 1121-1132.



| Cell line | GW4869 sensitivity[1] | Characteristics | | | | PS status[2] |
|---|---|---|---|---|---|---|
| | | Translocation | Target | *RAS* | *TP53* | |
| JJN3 | Yes | t(14;16) | *MAF* | mut | abn | High |
| RPMI-8226 | Yes | t(14;16) | *MAF* | mut | abn | High |
| NCI-H929 | Yes | t(4;14) | *NSD2/FGFR3* | mut | wt | High |
| OPM2 | Yes | t(4;14) | *NSD2/FGFR3* | wt | abn | High |
| ANBL6 | Weak | t(14;16) | *MAF* | wt | abn | High |
| LP1 | Weak | t(4;14) | *NSD2/FGFR3* | wt | abn | Moderate |

| | | | | | | |
|---|---|---|---|---|---|---|
| KMS18 | No | t(4;14) | *NSD2/FGFR3* | n.a. | abn | High |
| U266 | No | t(11;14) | *CCND1* | wt | abn | Moderate |
| MM.1S | No | t(14;16) | *MAF* | mut | wt | Moderate |
| KMS11 | No | t(4;14) | *NSD2/FGFR3* | wt | abn | Moderate |
| JIM1 | No | t(4;14) | *NSD2/FGFR3* | n.a. | n.a. | Low |
| WL-2 | No | n.a. | n.a. | n.a. | n.a. | Low |

**Table I. Summary of surface PS expression and GW4869 sensitivity for MM cell lines.**

[1]GW4869 sensitive cell lines are those that show more than 50% cell death (normalised to vehicle control) when treated with 5 μM GW4869 for 72 h. Cell lines with weak sensitivity are those that show between 25 and 50% cell death, and insensitive cell lines display less than 25% GW4869-dependent cell death. Data for cell line characteristics is derived from Teoh *et al* (2014), Moreaux, *et al* (2011) and Ronchetti, *et al* (2001). [2]PS status: geometric mean fluorescence intensity values > 1000 = High, 100 – 1000 = Moderate, 25 – 100 = Low, 0 – 25 = None.

abn, abnormal; mut, mutated; n.a., not available; PS, phosphatidylserine; wt, wildtype.

| | ***n*** | **t half (s)** | **p-value** | **Mobile** | **p-value** |
|---|---|---|---|---|---|
| **OPM2** | | | | | |
| DMSO | 36 | 2.67 [1.53] | | 0.91 [0.15] | |
| GW4869 | 41 | 4.87 [4.12] | 0.0035** | 0.64 [0.31] | <0.0001**** |
| **RPMI-8226** | | | | | |
| DMSO | 49 | 4.40 [2.48] | | 0.85 [0.21] | |
| GW4869 | 50 | 7.10 [5.49] | 0.0023** | 0.69 [0.31] | 0.0036** |

**Table II. FRAP values for OPM2 and RPMI-8226 cell lines.**

Values in square brackets denote standard deviation. p-values calculated using a two-tailed t-test.

DMSO, dimethyl sulphoxide; FRAP, Fluorescence recovery after photobleaching

## FIGURE LEGENDS

**Figure 1. GW4869 is selectively cytotoxic to multiple myeloma (MM) cell lines.** (A) MM cell lines and (B) non-MM cells were incubated with serial diluted concentrations of GW4869 or equivalent levels of dimethyl sulphoxide (DMSO, vehicle control). After 72 h,

cells were harvested, stained with propidium iodide and assessed for cell viability by flow cytometry. Values are normalised to the no treatment control sample (data points are mean of n=3 replicates, error bars are ± SEM) (C) RPMI-8226 and OPM2 cell lines were treated with 5 μM GW4869 or DMSO for 8 and 24 h then assayed for caspase 3/7 activity (column heights are mean of n=3, error bars are ± SEM).

**Figure 2. GW4869 depletes CD138$^+$ MM cells in BMMNC primary cell cultures.** Bone marrow mononuclear cells (BMMNCs) derived from a patient with multiple myeloma (MM), were cultured for 24 h with medium alone or the indicated concentrations of dimethyl sulphoxide (DMSO, vehicle) or GW4869. The proportion of viable CD138$^+$ plasma cells was then determined by flow cytometry.

**Figure 3. GW4869 delays multiple myeloma (MM) cell growth in a xenograft model.** CD122$^+$ depleted MM-bearing NOD/SCID mice were treated daily with i.p. injections of 1.25 μg/g GW4869 (n=8) or dimethyl sulphoxide (DMSO) vehicle control (n=7). After two weeks, mice were culled and assessed for (A) serum lambda light chain levels by enzyme-linked immunosorbent assay or (B) the proportion of GFP$^+$ RPMI-8226 cells in the femur/tibia and lumbar spine (**p-value<0.01, n.s. not significant, two-tailed Mann-Whitney test). (C) Combined proportion of GFP$^+$ RPMI-8226 cells (DMSO normalised, *p-value<0.05, two-tailed Mann-Whitney). (D) Kaplan-Meier plots showing survival of MM-bearing mice treated daily with GW4869 (n=10) or DMSO vehicle control (n=9) until they succumbed to hind-limb paralysis or death (*p-value<0.05, two-tailed log-rank test, error bars are ± SEM).

**Figure 4. nSMase2 expression and correlation with GW4869-induced cytotoxicity.** (A) Western blot assessing nSMase2 and actin expression in multiple myeloma (MM) and non-MM cell lines. (B) qPCR analysis of *SMPD3* (*NSMASE2*) mRNA expression in MM and non-MM cells. Solid black columns represent non-MM cells and chequered columns represent MM cell lines (column heights are mean of n=3 replicates, error bars are ± SEM) (C) RPMI-8226 and OPM2 cells were treated with dimethyl sulphoxide (DMSO, vehicle control) or GW4869 for the indicated time periods. Cells were then harvested and then assessed for sphingomyelin and ceramide levels (column heights are mean of n=3 replicates,

error bars are ± SEM, *p-value <0.05, ***p-value<0.001, two-tailed t-test). PBMCs, peripheral blood monoclonal cells.

**Figure 5. Reduced expression of nSMase2 and its effects on GW4869 mediated cytotoxicity.** (A) qPCR measuring the relative *SMPD3* mRNA levels between RPMI-8226 stably expressing an shRNA specific for *SMPD3* and a scrambled shRNA control (column heights are mean of n=4 replicates, error bars are ± SEM). (B) anti-nSMase2 and and anti-actin Western blot of control and *SMPD3* shRNA stable transfectants. Numbers denote normalized densitometry values as calculated by ImageJ. (C) Growth competition assay measuring the ratio of $GFP^+$ shRNA-expressing cells versus non-transduced $GFP^-$ cells over time. (D) RPMI-8226 cells stably expressing an shRNA specific for *SMPD3* or a scrambled control, were treated with 5 μM GW4869 or vehicle control (dimethyl sulphoxide) for 48 h, then assessed for cell viability by propidium iodide staining and flow cytometry (column heights are mean of n=3 replicates, error bars are ± SEM, n.s. not significant, two-tailed t-test).

**Figure 6. GW4869 localizes to the cell membrane of multiple myeloma cells.** Confocal microscopy analysis of RPMI-8226 cells. (A) Cells were pre-treated with dimethyl sulphoxide (DMSO; top panel) or GW4869 (bottom panel) for 8 h and then stained for CD138 (green channel). Blue channel shows GW4869-specific fluorescence. (B) Cells were pre-treated with DMSO (top panel) or GW4869 (bottom panel) and then stained for CD120b (green channel). Blue channel denotes GW4869-specific fluorescence.

**Figure 7. GW4869-treated cells show reduced membrane fluidity.** (A) Mean fluorescence recovery after photobleaching (FRAP) curves for dimethyl sulphoxide (DMSO)- and GW4869-treated OPM2 cells calculated using EasyFRAP software as described in the Methods section. (B) Representative images of DiI-stained OPM2 cells at various times points during FRAP acquisition.

**Figure 8. GW4869 binds to anionic phospholipids.** (A) Phospholipid binding assay testing the ability of GW4869 to be absorbed onto monolayers of various lipid species (column heights are mean of n=3 replicates, error bars are ± SEM) (B) Testing of GW4869 binding to liposomes composed of PC only, as well as mixed liposomes composed of PC and PS or PC

and PA (3:1 ratio of PC to anionic lipid; column heights are mean of n=3 replicates, error bars are ± SEM). PA, phosphatidic acid; PC, 1,2-dioleoyl-*sn*-glycero-3-phosphatidylcholine; PE, 1-palmitoyl-2-oleoyl-*sn*-glycero-3-phosphatidylethanolamine; PG, phosphatidylglycerol; PI, phosphatidylinositol; PS, 1-palmitoyl-2-oleoyl-*sn*-glycero-3-phosphatidylserine.

**Figure 9. Multiple myeloma (MM) cells incorporate higher levels of GW4869 than non-MM cells.** Cells were incubated with 5 μM GW4869 or dimethyl sulphoxide (DMSO)under normal tissue culture conditions. After 4 h, cells were harvested and then assessed by flow cytometry for GW4869 uptake. (A) OPM2 and (B) Daudi histogram overlays. Continuous line represents GW4869-treated cells and solid grey histogram represents DMSO-treated cells. (C) Geometric mean fluorescence intensity (geoMFI) for cells treated with GW4869. Solid black columns represent non-MM cells and chequered columns represent MM cell lines (column heights are mean of n=3 replicates, error bars are ± SEM) (D) NOD/SCID mice bearing $GFP^+$ RPMI-8226 myeloma, were treated daily with DMSO or GW4869. At day 10 of treatment, bone marrow cells were harvested and $GFP^+$ RPMI-8226 cells were assessed for GW4869-specific fluorescence by flow cytometry. PBMCs, peripheral blood monoclonal cells.

**Figure 10. Multiple myeloma (MM) cells express cell surface phosphatidylserine (PS).** (A) MM cells propagated *in vitro* or in NOD/SCID mice bearing $GFP^+$ RPMI-8226 myeloma and (B) non-MM cells were stained with anti-PS mAb (continuous line) or IgG2a isotype control (solid grey histogram) and then assessed by flow cytometry. (C) OPM2 cells were-treated with 25 μg/ml mitomycin C (mito. C) or vehicle control for 18 h and then assessed for surface PS expression. Continuous line represents vehicle control-treated cells, dashed line represents mitomycin C-treated cells and the solid grey histogram represents the isotype control. (D, E) Cell surface PS expression on primary MM cells from two patients (D as an example of a high expressor and E as a low expressor). MM cells were gated according to dual expression of CD38 and CD138 and then analysed for cell surface PS. Continuous line represents anti-PS stained cells and solid grey histogram denotes IgG2a isotype control.

**Figure 11. Brefeldin A reduces exoplasmic PS levels and inhibits GW4869 cytotoxicity.** (A) MM cells were pre-treated with BFA or EtOH vehicle control for 4 h and then stained for

PS (left panel) or treated with 5 μM GW4869 for 12 h (right panel) before assessment by flow cytometry. Data shows geometric mean fluorescence intensity values expressed as a percentage of the vehicle control (column heights are mean of n=3 replicates, error bars are ± SEM, *p-value<0.05, **p-value<0.01, two-tailed one sample t-test). (B) RPMI-8226 cells and OPM2 cells were pre-treated BFA or EtOH vehicle control for 4 h, and then treated with 5 μM GW4869 or DMSO for 12 h. Cells were then harvested and cell viability was determined by flow cytometry. Per cent viability was normalised to the DMSO control samples (column heights are mean of n=3 replicates, error bars are ± SEM, *p-value<0.05, ns: not significant, two-tailed t-test). BFA, brefeldin A; DMSO, dimethyl sulhoxide; EtOH, ethanol; geoMFI, geometric mean fluorescence intensity; PS, phosphatidylserine.

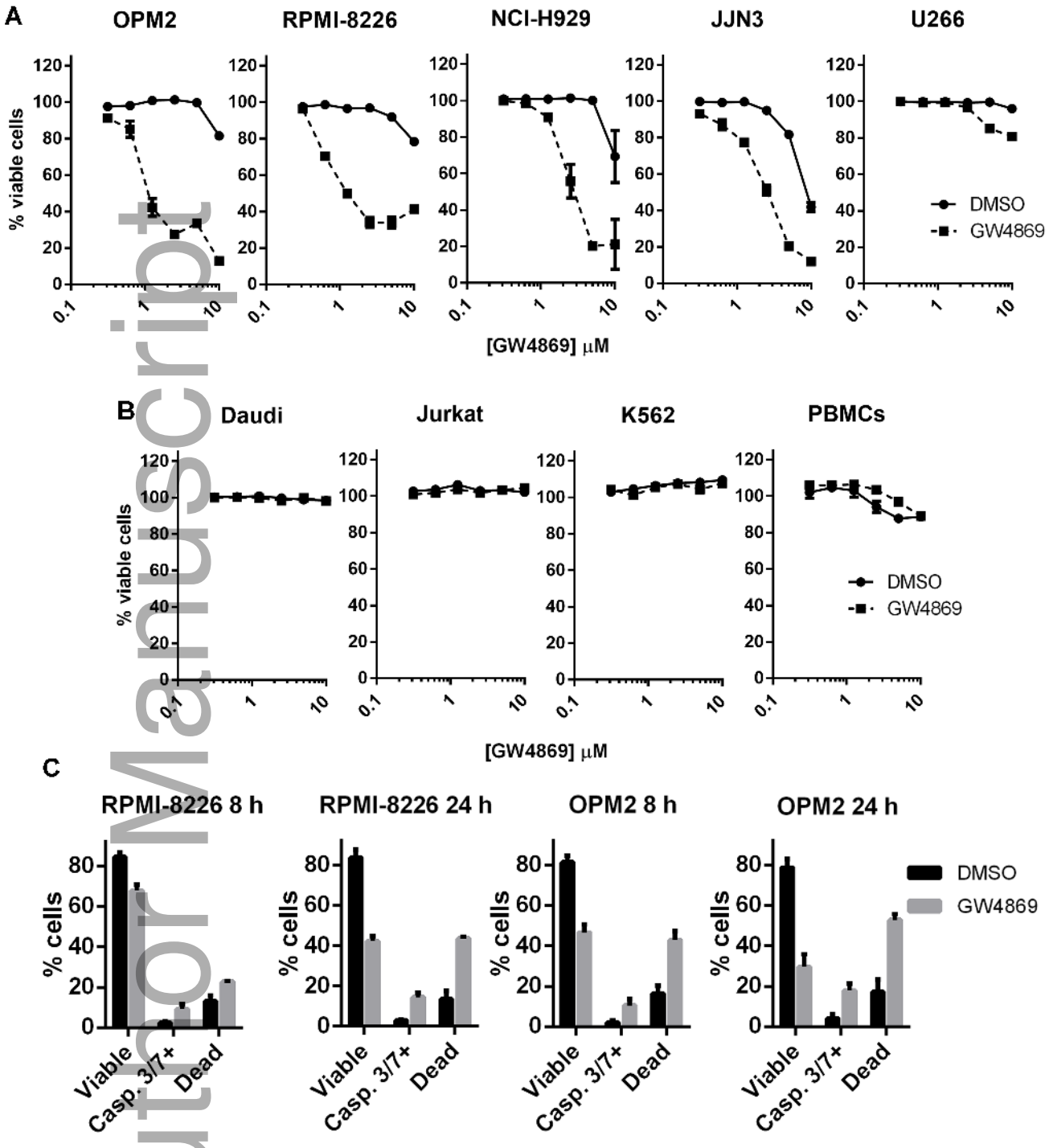


bjh_14561_f1.tif

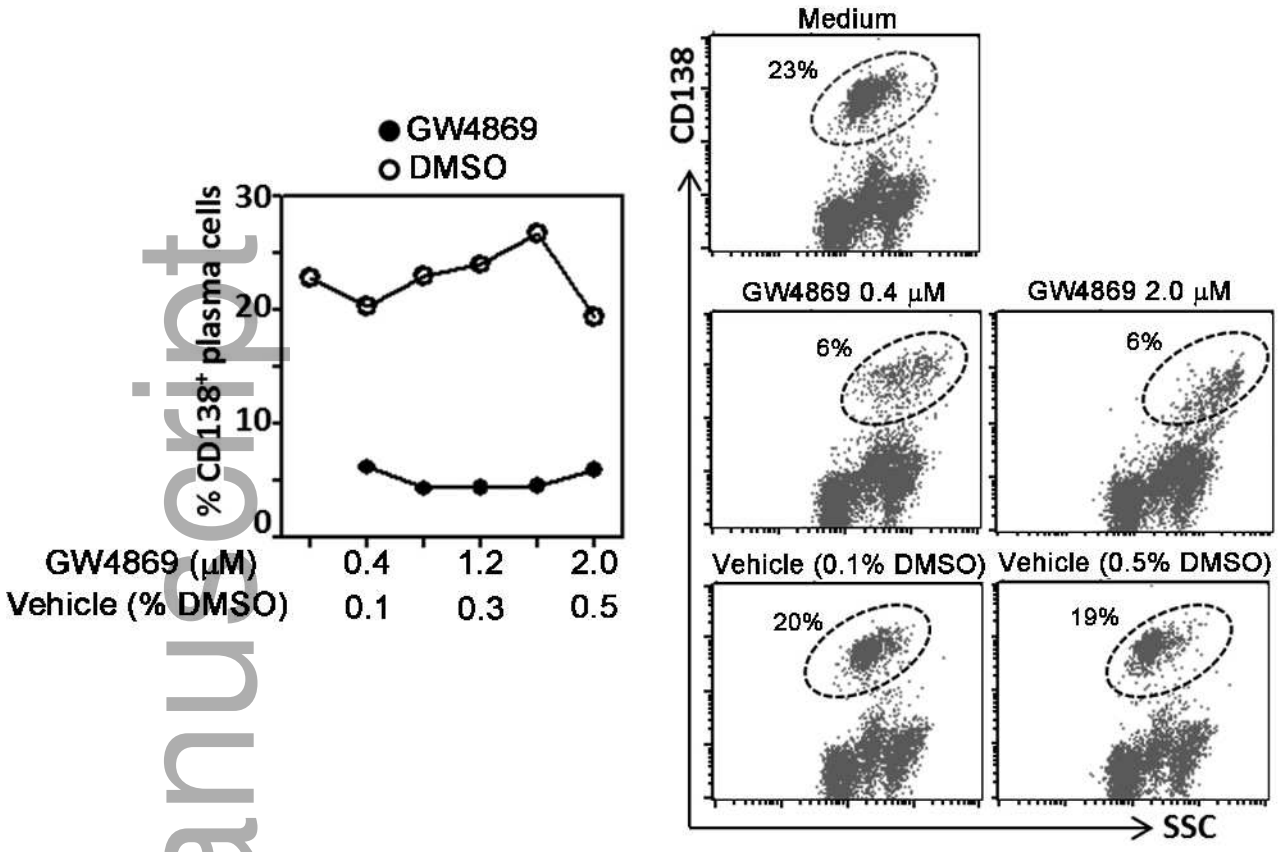


bjh_14561_f2.tif

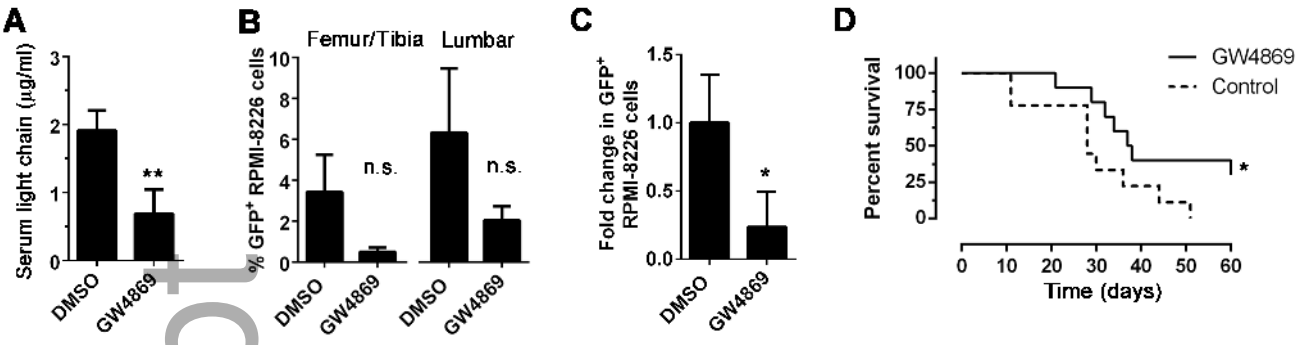


bjh_14561_f3.tif

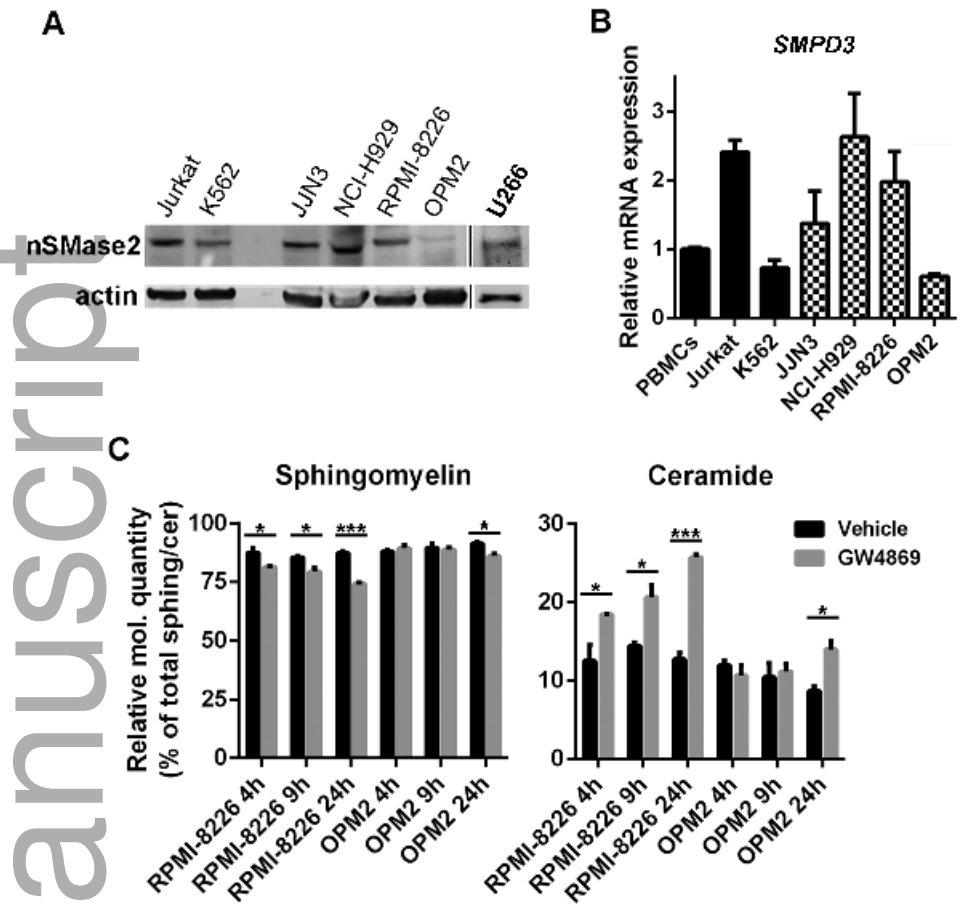


bjh_14561_f4.tif

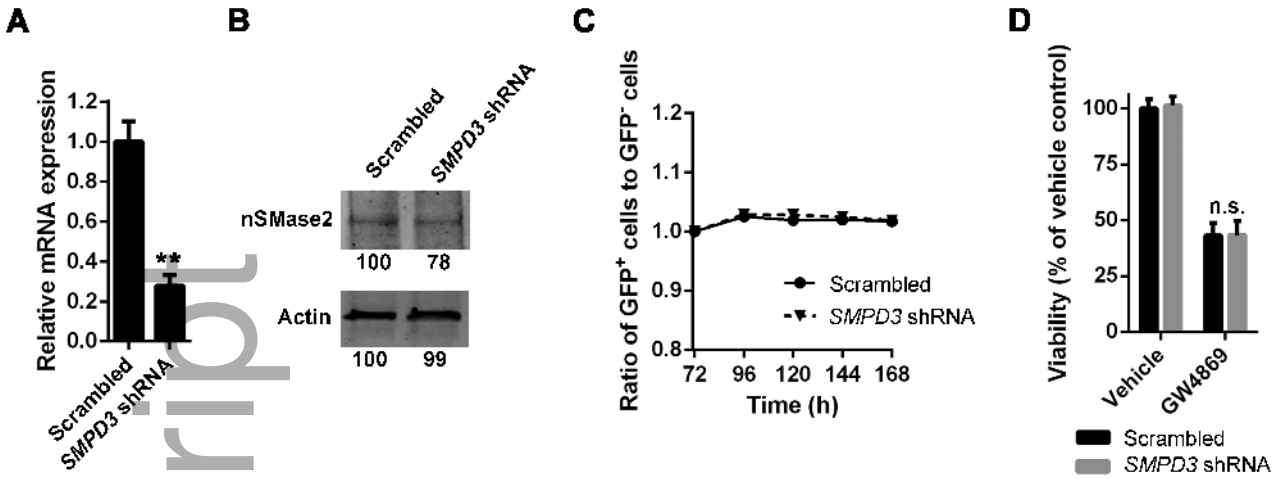


bjh_14561_f5.tif

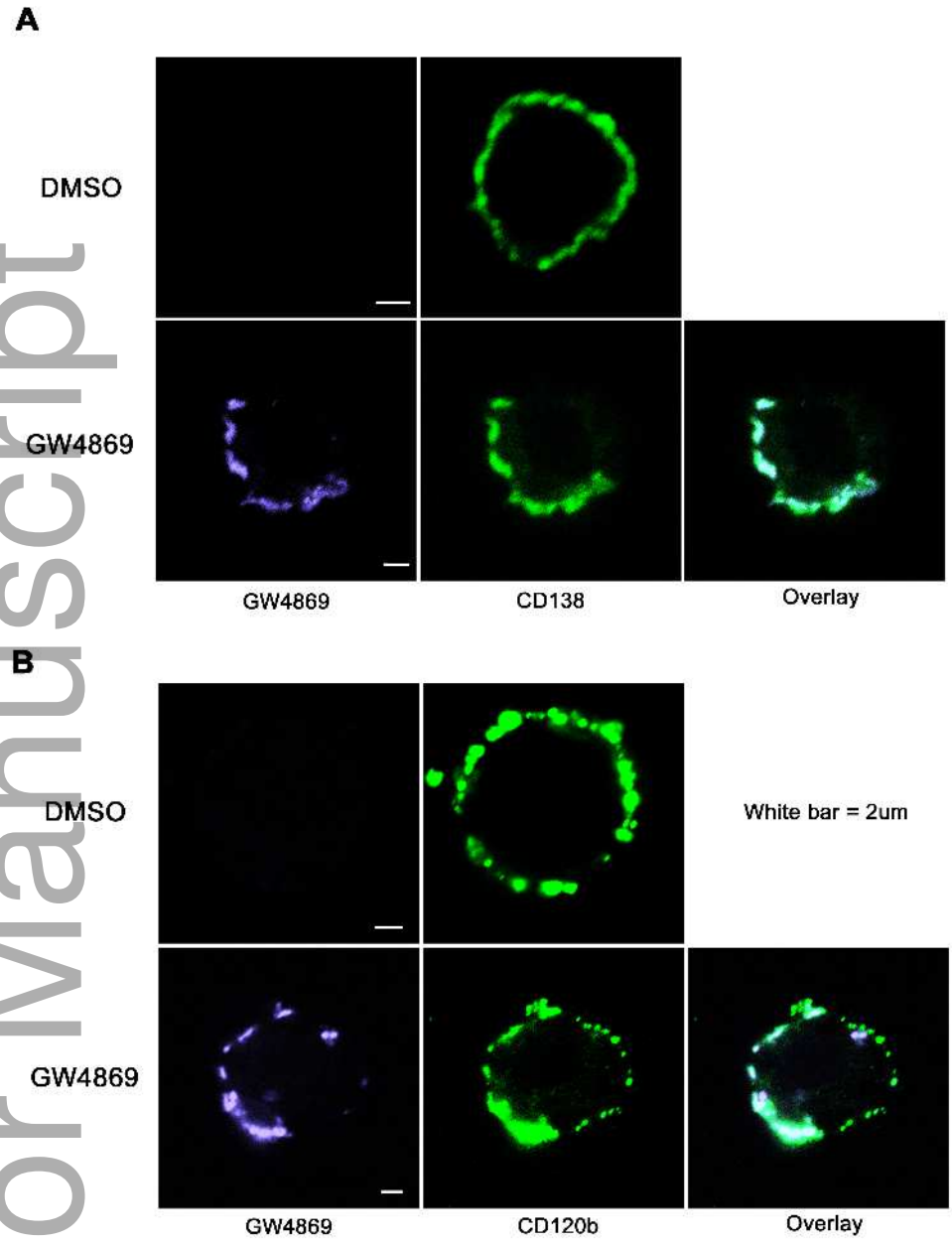


bjh_14561_f6.tif

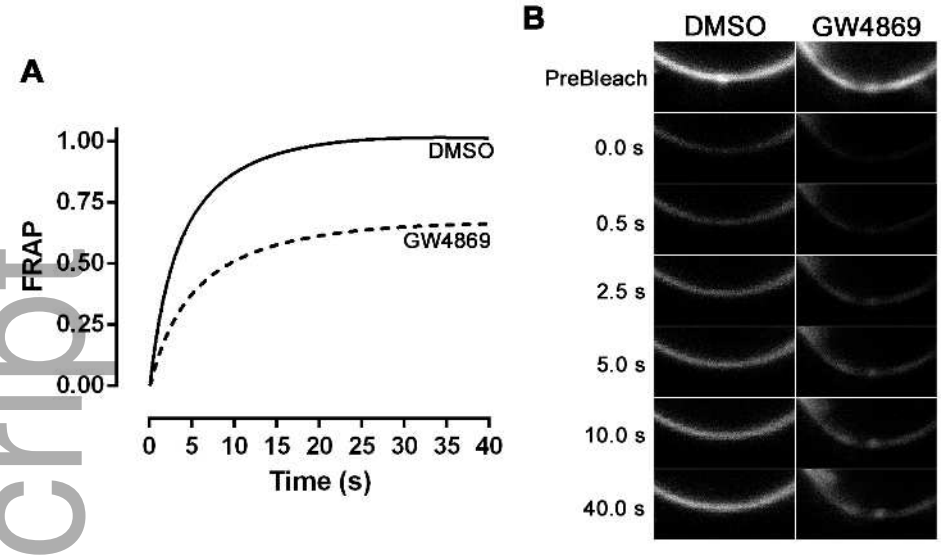


bjh_14561_f7.tif

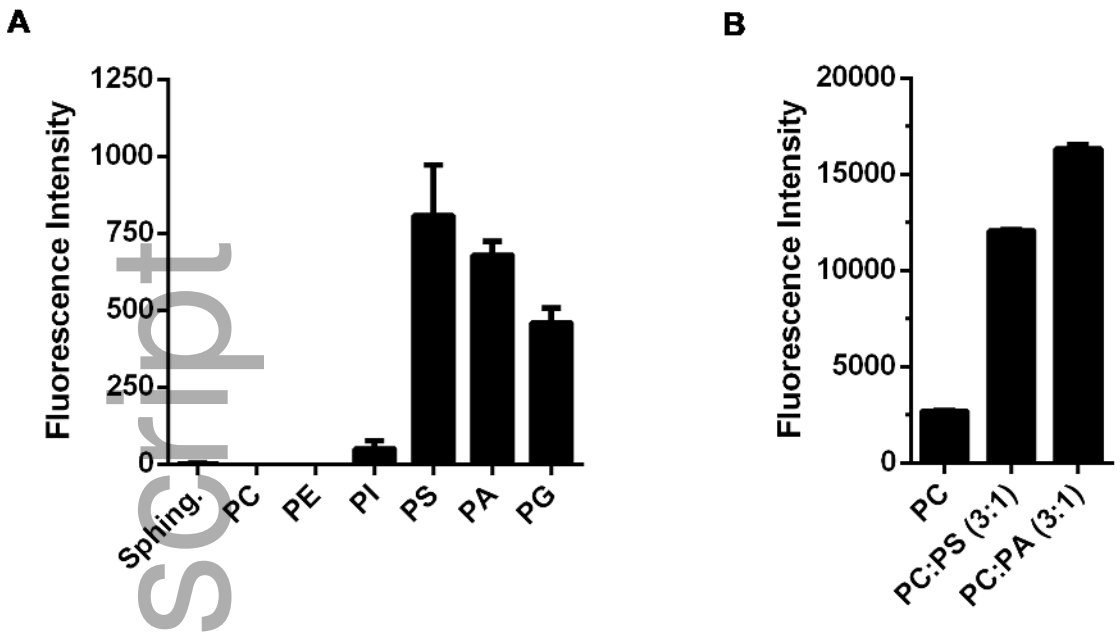


bjh_14561_f8.tif

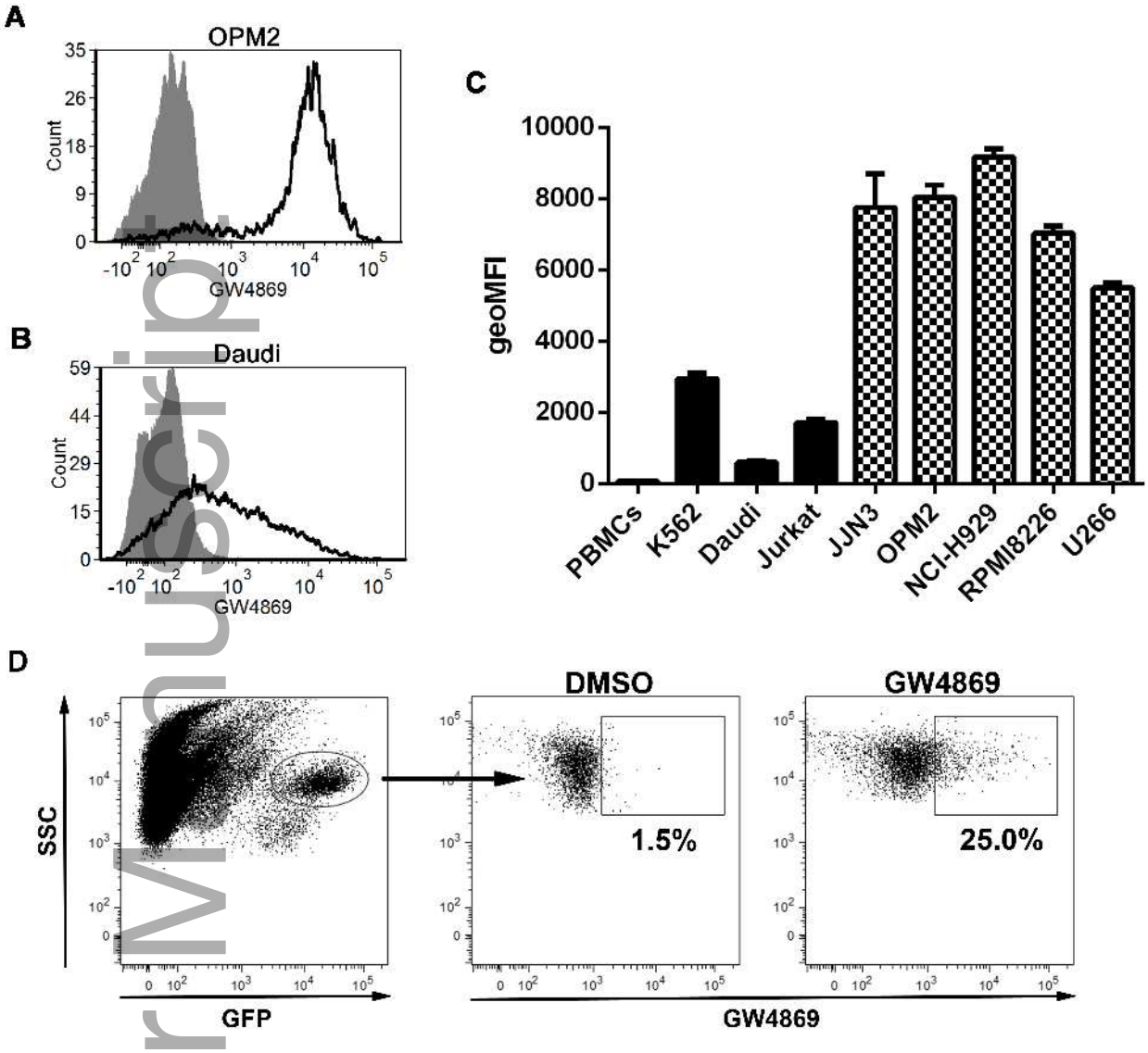


bjh_14561_f9.tif

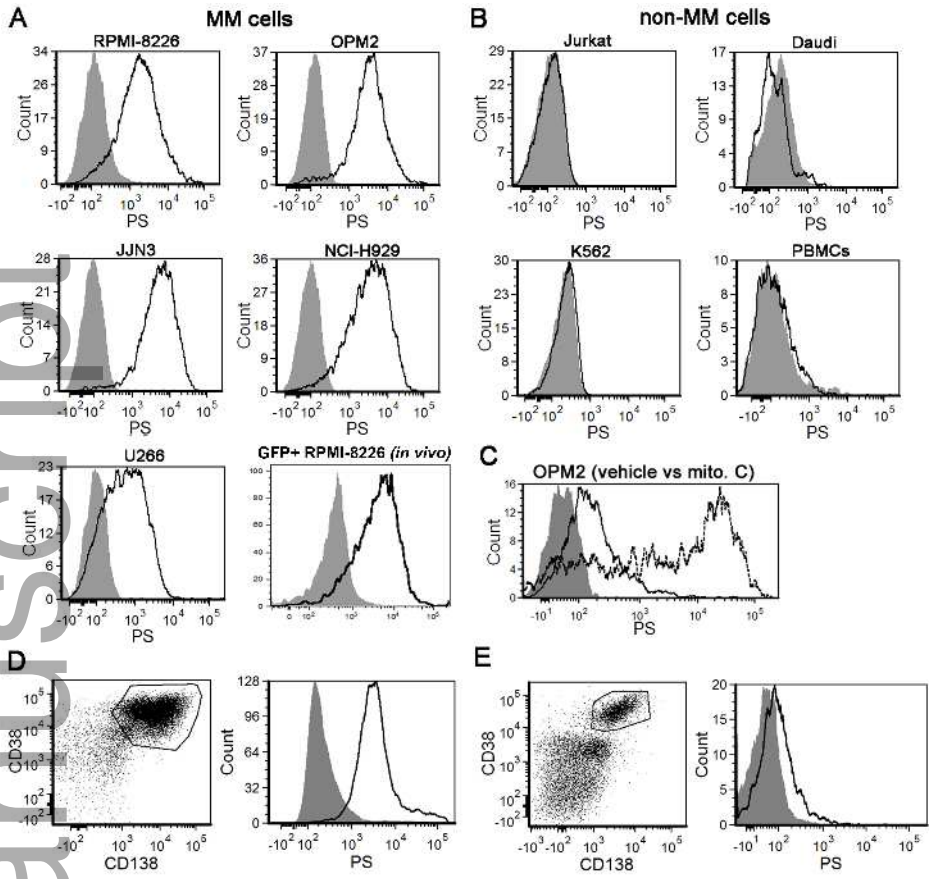


bjh_14561_f10.tif

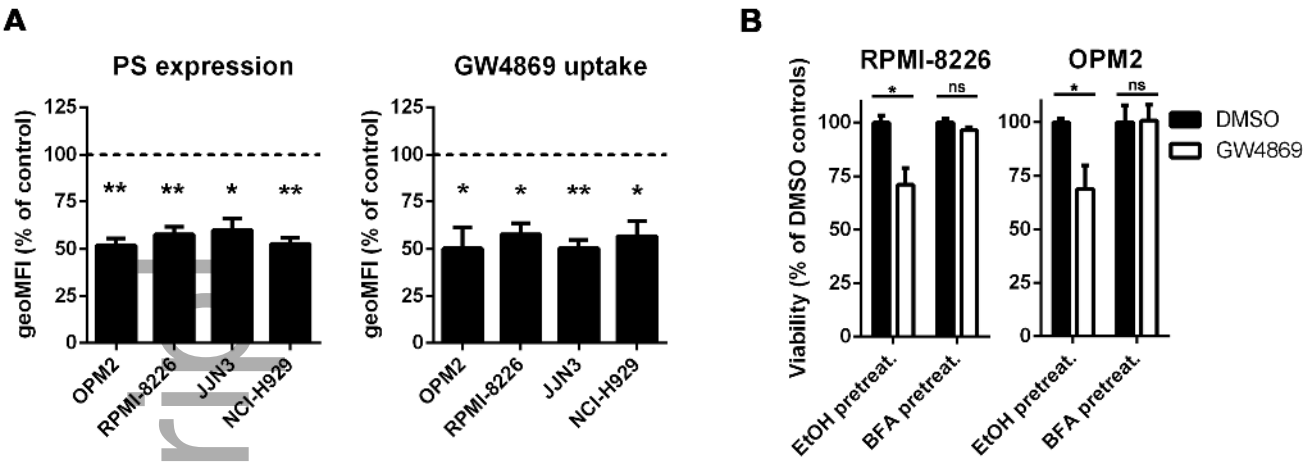


bjh_14561_f11.tif